

# APPLICATIONS OF MAGNETIC HELICAL NANOMOTORS



Debayan Dasgupta



# Outline

Micro-rheology using nanomotors

Probing the cancer microenvironment

Nanomotors in real world



# Helical Swimmers

Helix satisfies the non-reciprocal condition needed to swim at low Reynolds number

Navier - Stokes:

$$-\nabla p + \eta \nabla^2 \vec{v} = \rho \frac{\partial \vec{v}}{\partial t} + \rho (\vec{v} \cdot \nabla) \vec{v}$$

If  $Q \ll 1$ :

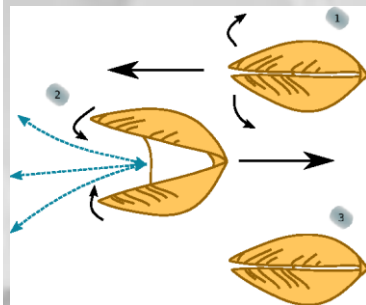
Time doesn't matter. The pattern of motion is the same, whether slow or fast, whether forward or backward in time.

The Scallop Theorem

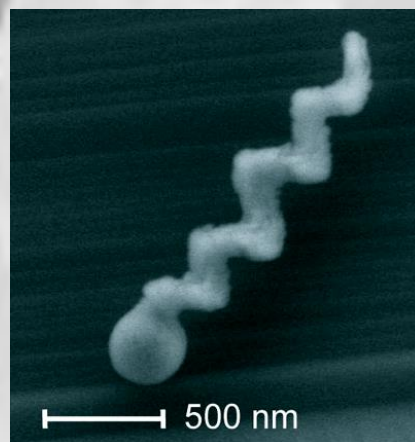


Figure 6

American Journal of Physics 45, 3 (1977)

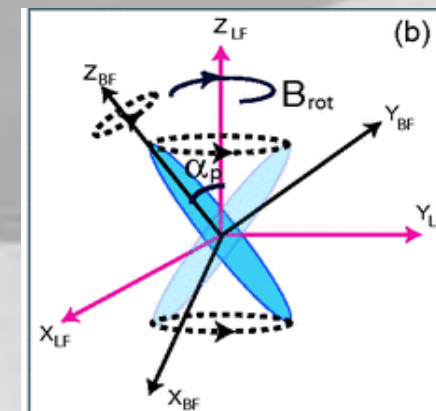


Glancing Angle Deposition to fabricate helix



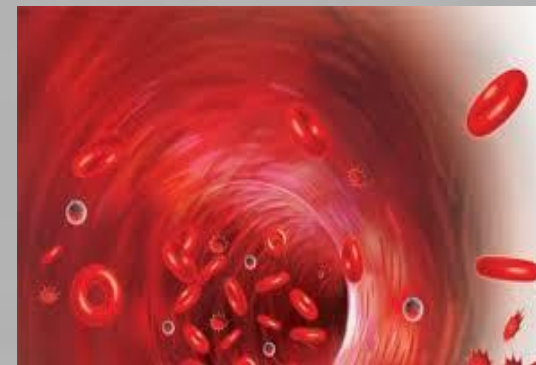
Nano Lett. 2009, 9, 6, 2243-2245

Dynamics of nanomotors

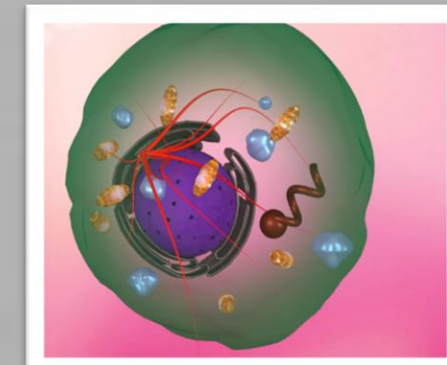


Phys. Chem. Chem. Phys., 2013, 15, 10817-10823

Applications in Biology

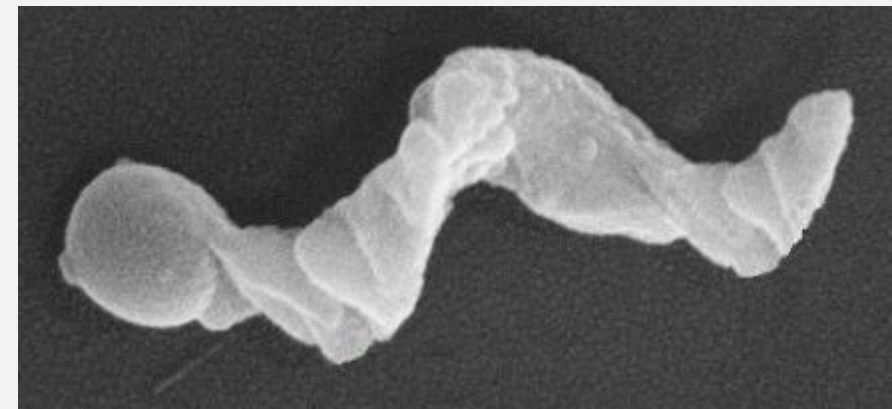
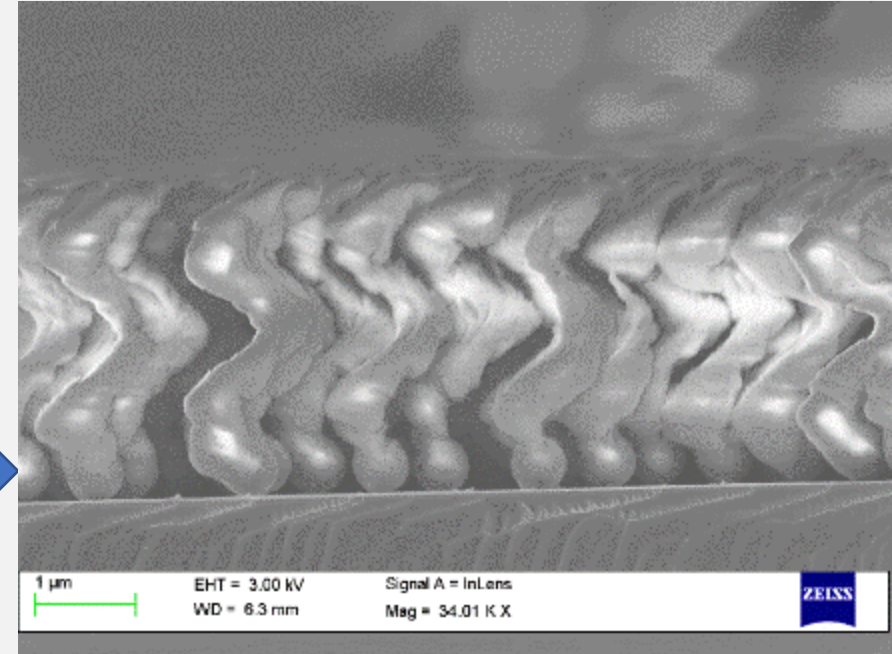
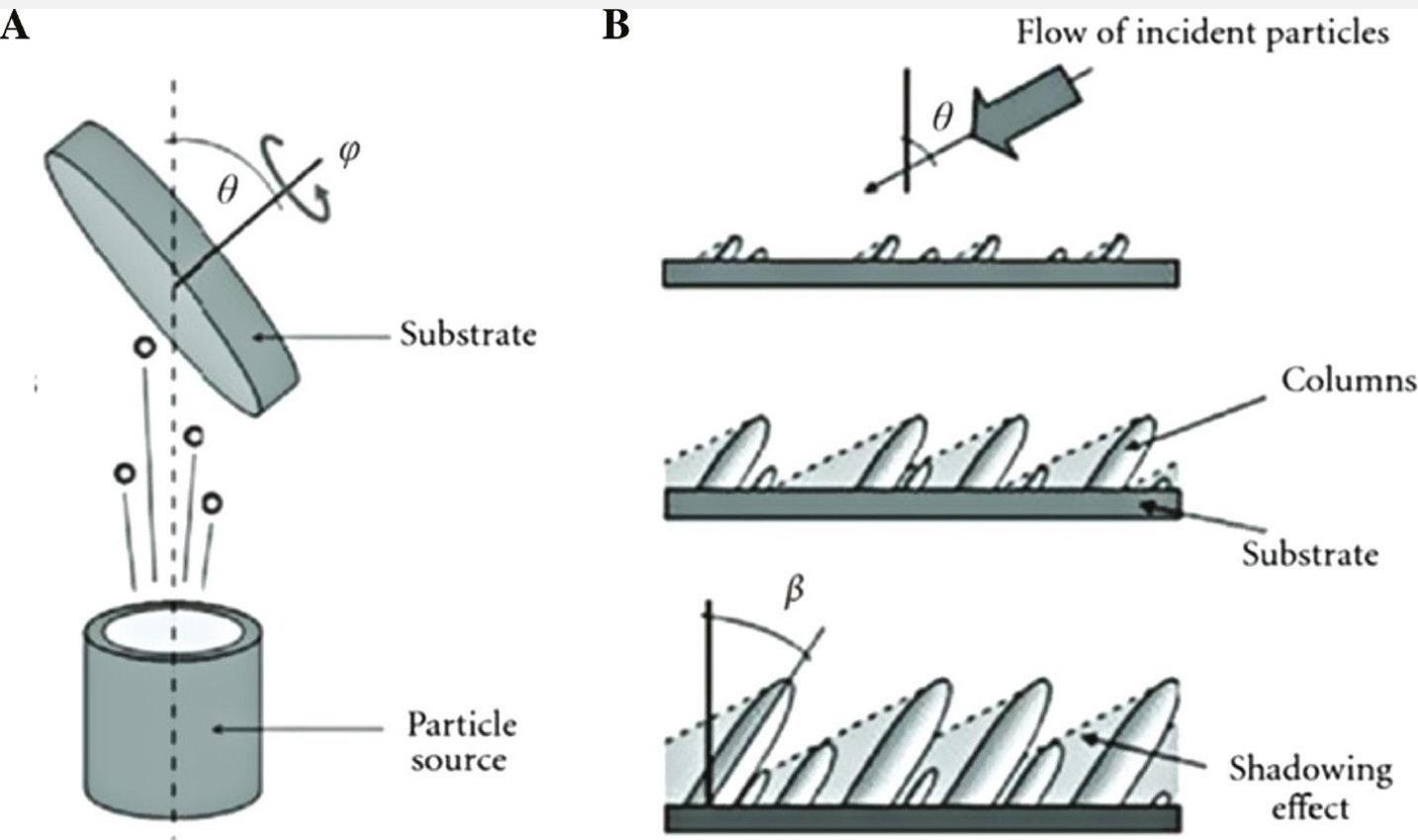


Nano Lett. 2014, 14, 4, 1968-1975

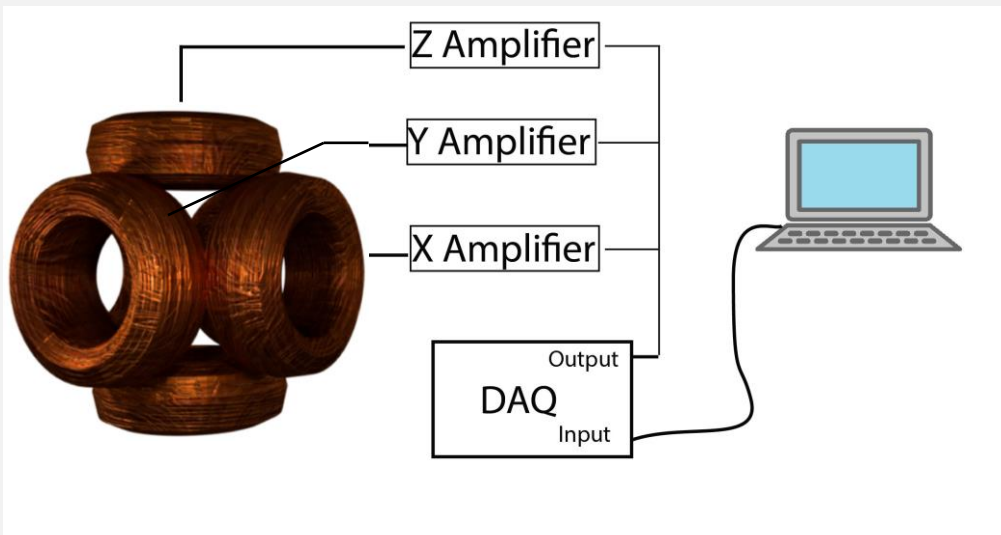
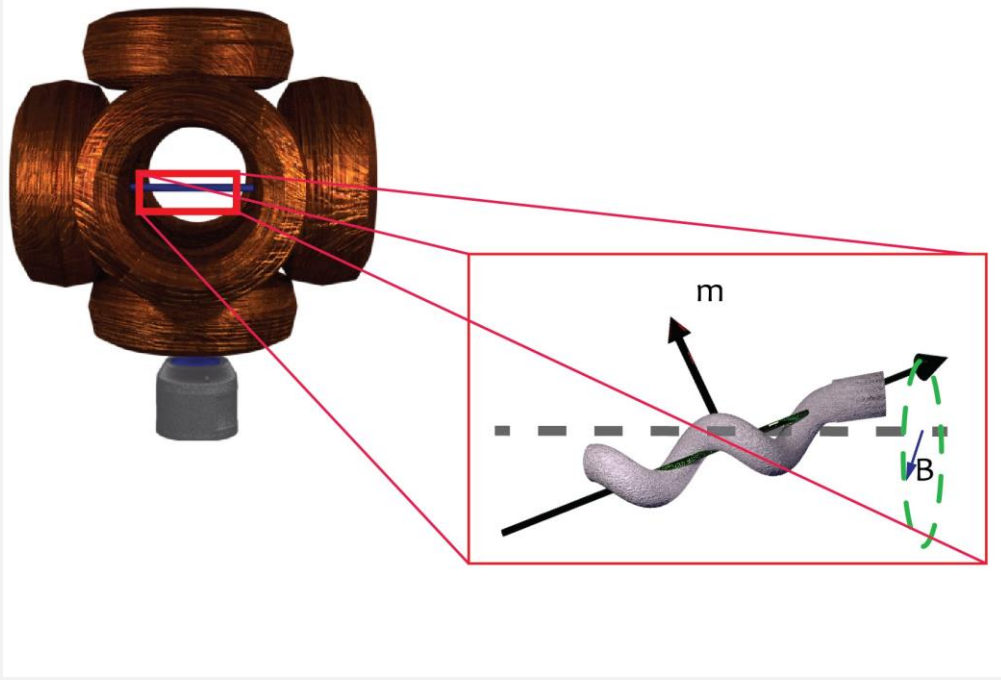


Adv. Mater. 2018, 30, 1800429

# Fabrication of nanomotors: Glancing Angle Deposition (GLAD)



# The setup



## Micro-rheology using nanomotors

- Localized viscosity measurement using nanomotors
- Viscosity measurement in Newtonian and non-Newtonian fluids
- Viscosity measurement in fluids whose property changes in real-time
- Viscosity measurement in miscible fluids

## Probing the cancer microenvironment

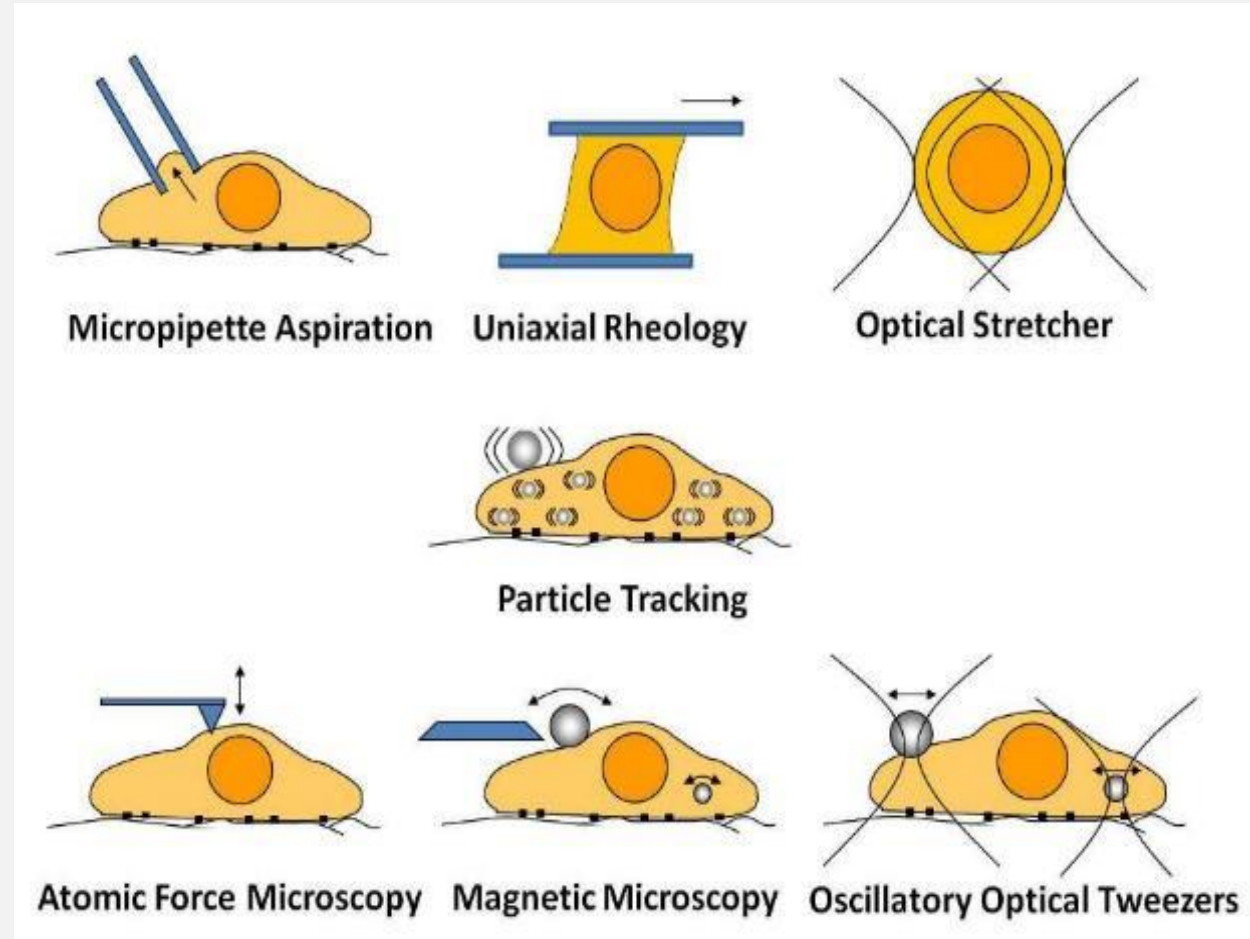
## Nanomotors in real world



# Microrheology using nanomotors: Advantages

Compared to present microrheology techniques:

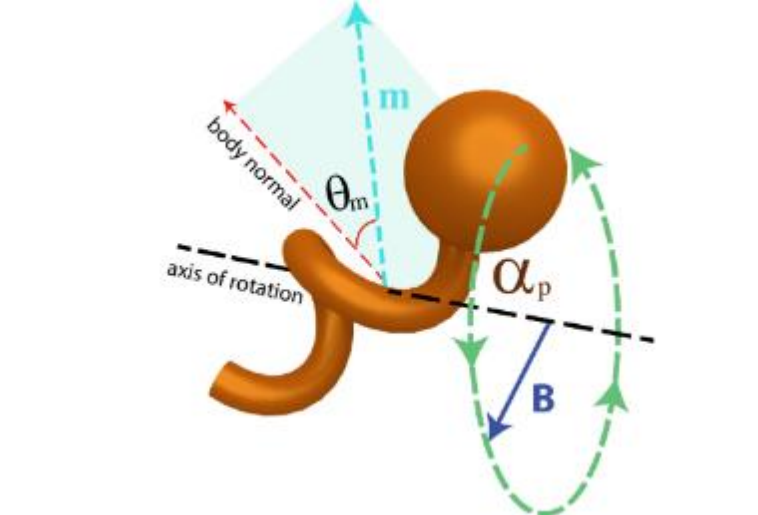
- Faster
- Measure local heterogeneity
- Higher spatio-temporal resolution
- Ease of creating a spatio-temporal map of viscosity in 3D



Wei, Ming-Tzo, "Microrheology of soft matter and living cells in equilibrium and non-equilibrium systems" (2014).Theses and Dissertations.Paper 1666

# Microrheology using nanomotors: Technique

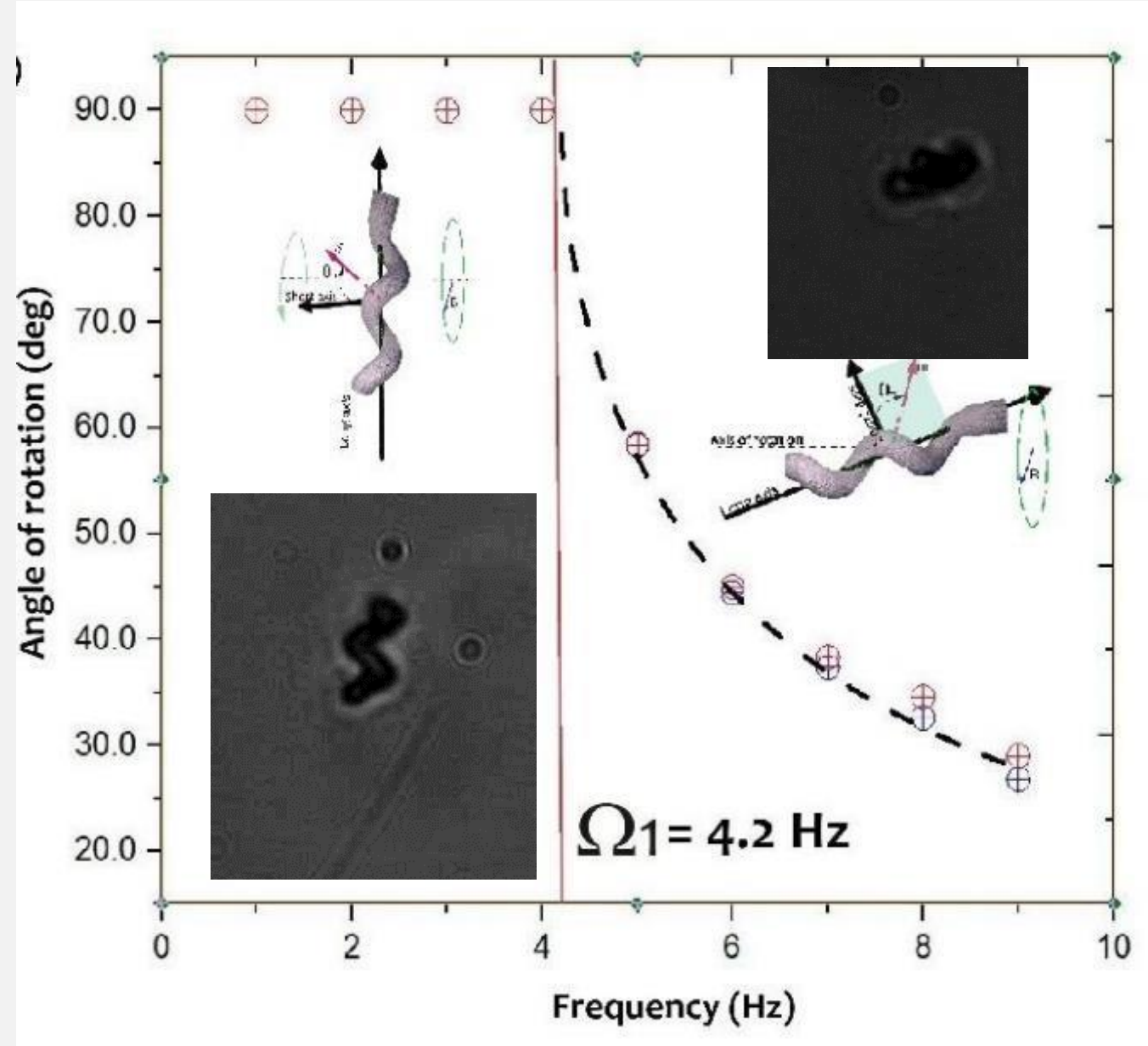
## How is viscosity measured



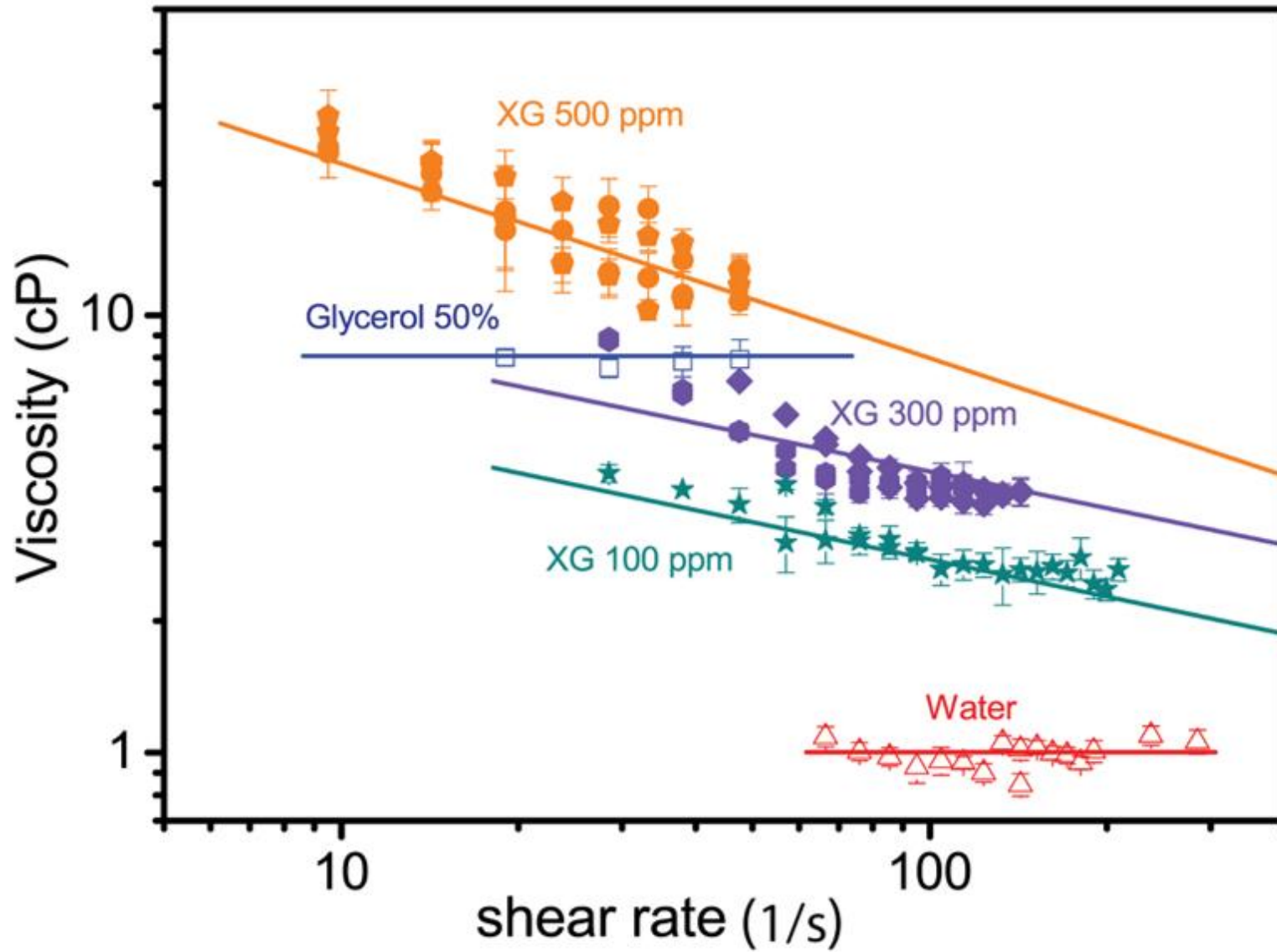
$$\alpha_p = \sin^{-1} \left( \frac{m B \sin(\theta_m)}{2\pi\eta f_s \Omega_B} \right)$$



$$\eta = \frac{m B \sin(\theta_m)}{2\pi f_s \Omega_B \sin(\alpha_p)}$$



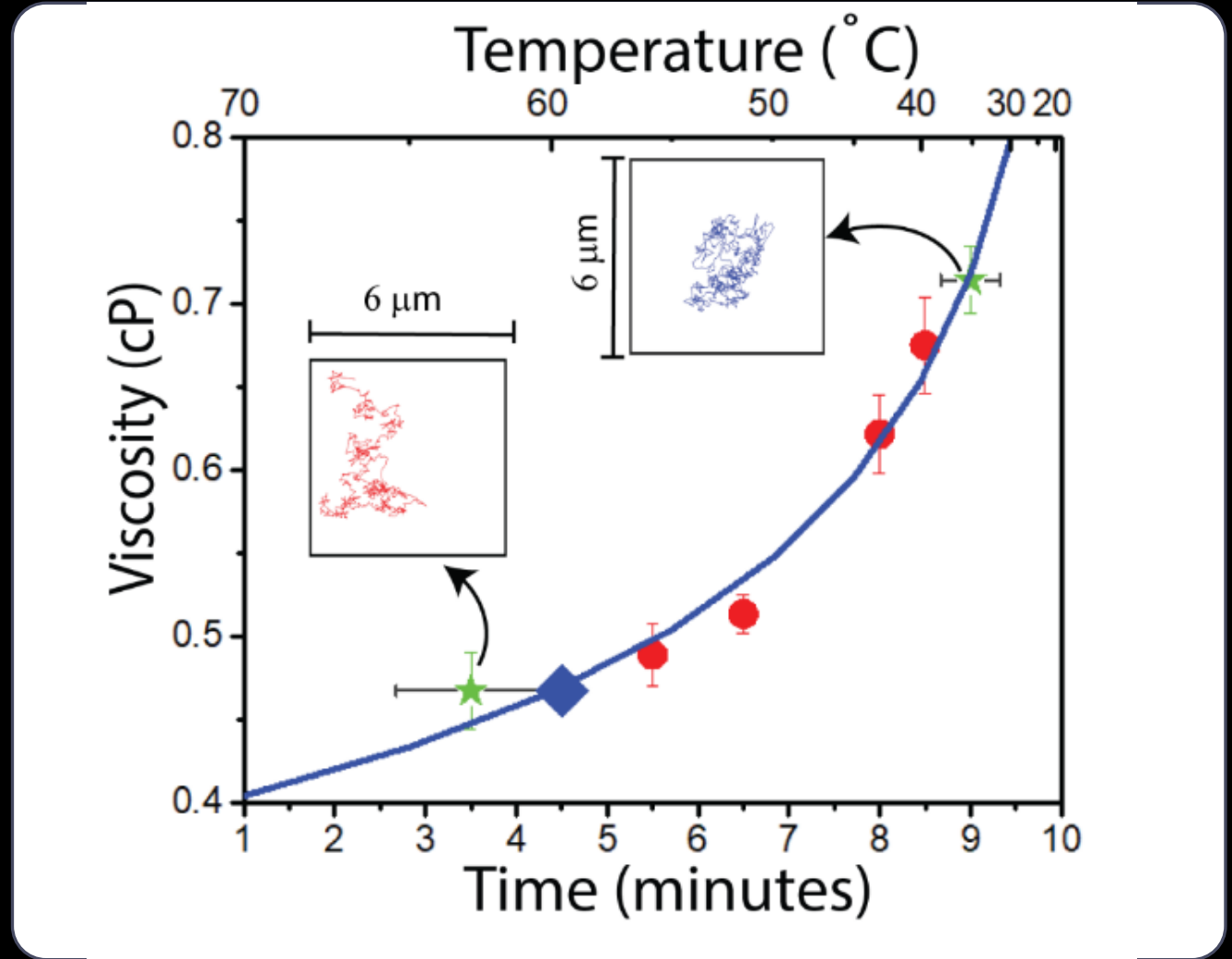




Newtonian and non-Newtonian fluids

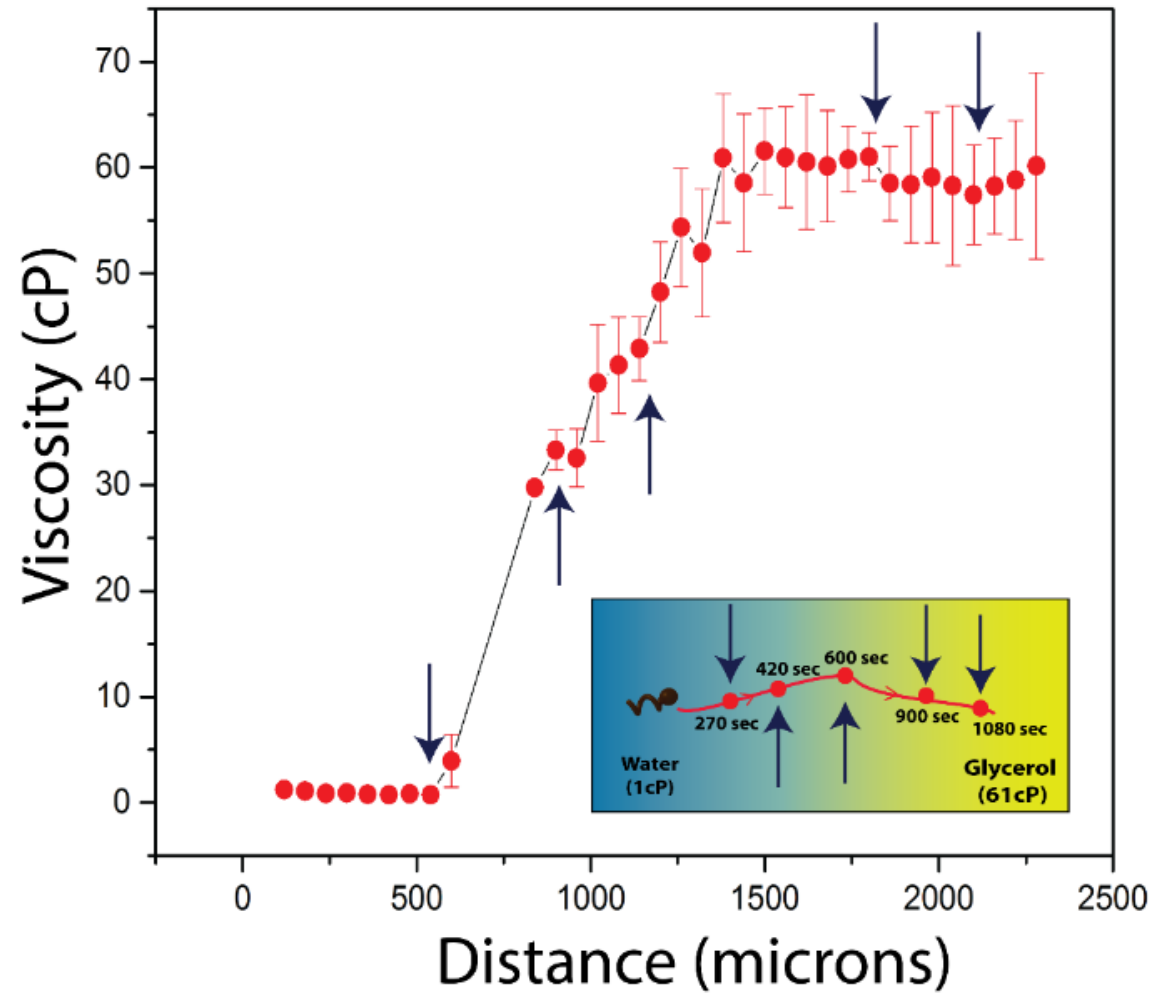
# Change in viscosity with time

- Heated water was allowed to cool down
- Temperature measured with IR thermometer – correlated with Brownian motion of beads.



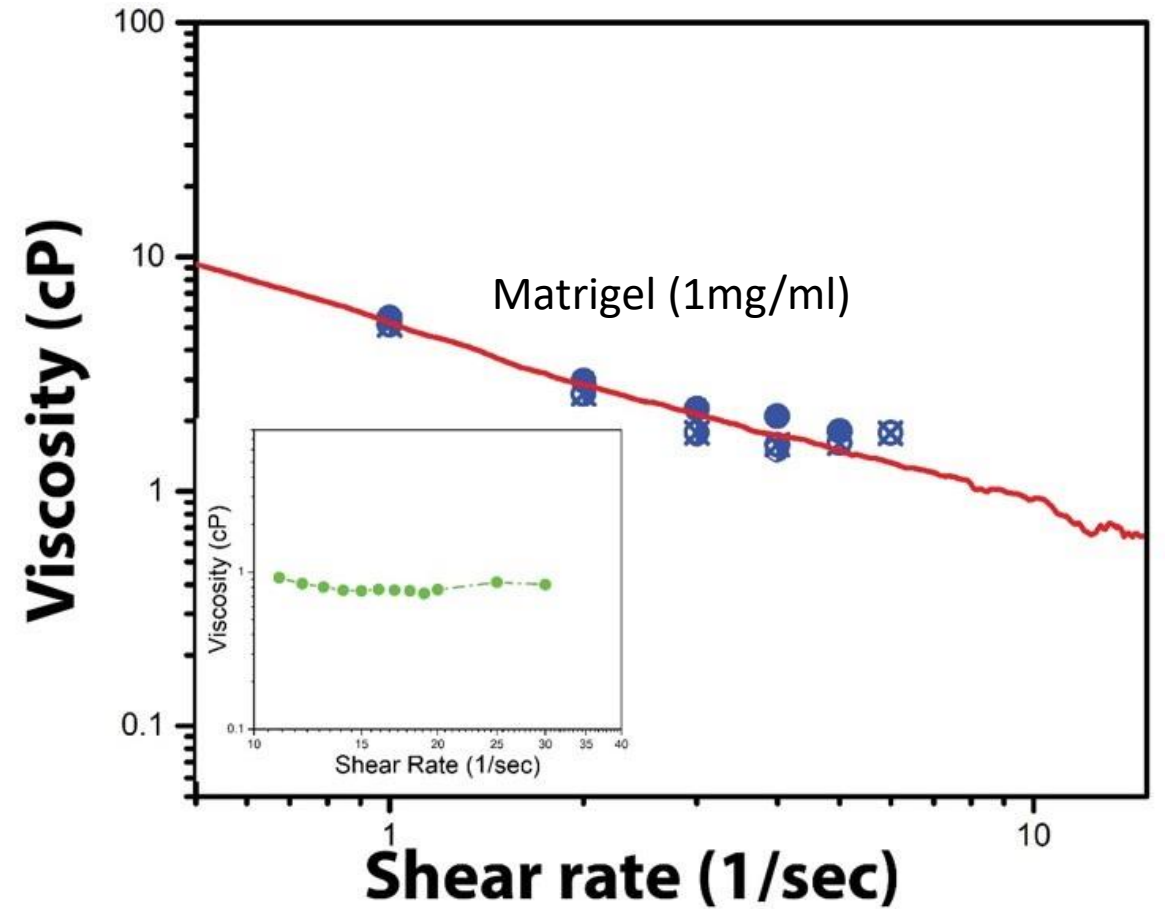
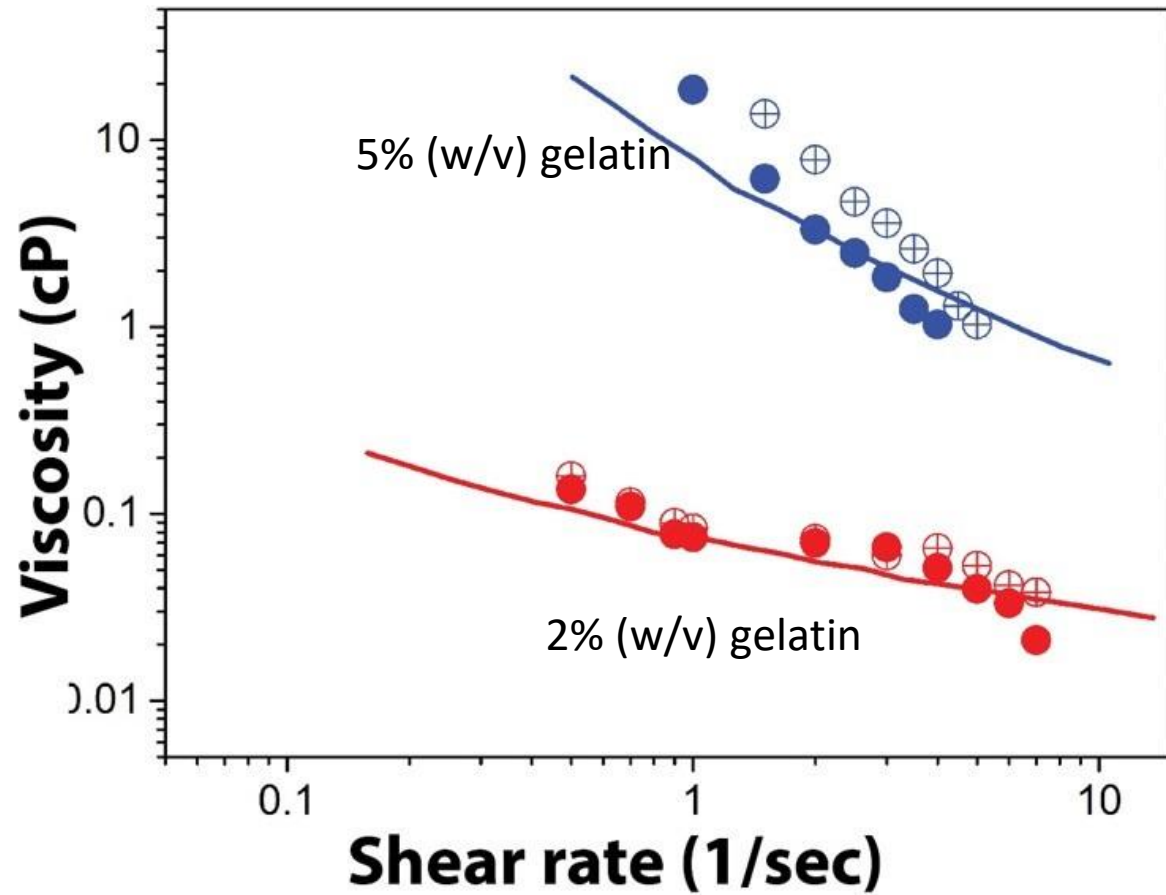
# Spatial change in viscosity

- Nanomotor was driven from DI water towards glycerol.
- Nanomotor was faster than the mixing time of 60 cP glycerol and water.





# Rheology in Biofluids



**Microrheology  
using  
nanomotors**

Measure viscosity in Newtonian and non-Newtonian fluids with high spatio-temporal accuracy.



Viscosity map of dynamic fluids

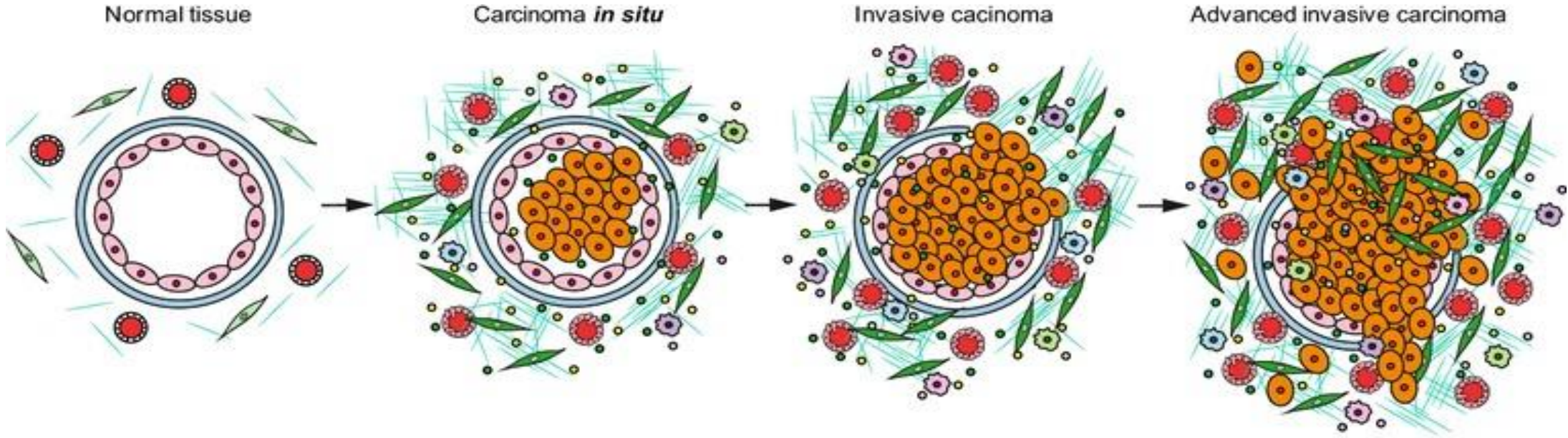
## Micro-rheology using nanomotors

## Probing the cancer microenvironment

- Maneuverability in tumor model
- Targeting cancer cells using changes in cancer microenvironment
- Discovery of new physico-chemical properties of cancer secreted matrix

## Nanomotors in real world





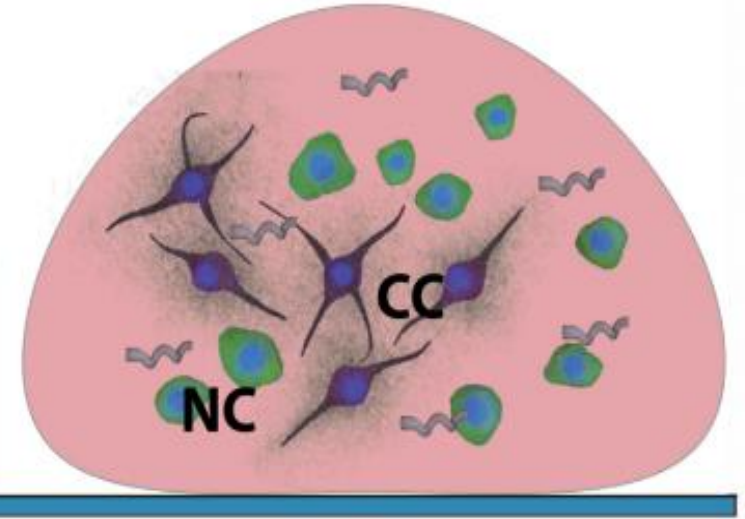
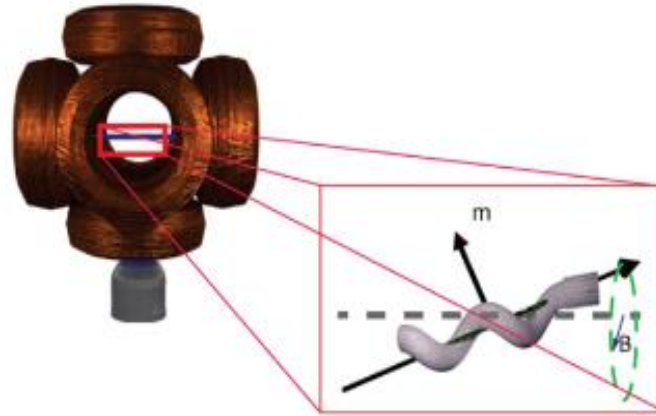
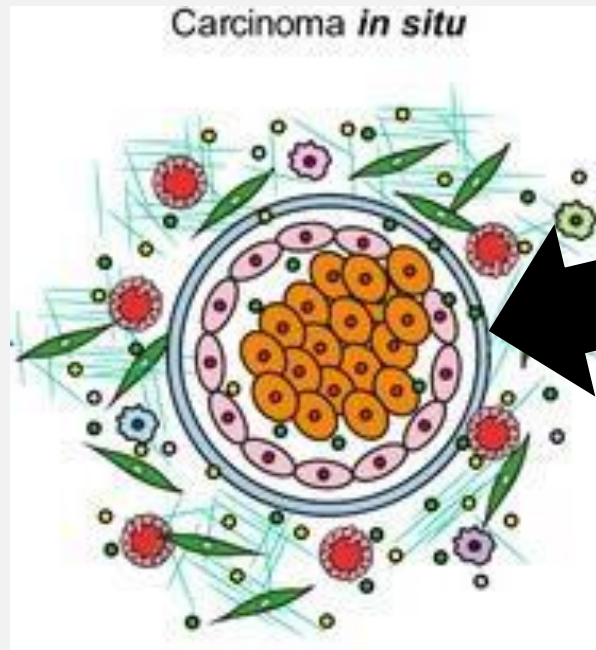
**Legend:**

Epithelial cell	ECM	Cancer cell	Cancer cell-derived secreted factors
Normal fibroblast	Basement membrane	CAF	CAF-derived secreted factors
Normal vasculature	Aberrant vasculature	Immune cells	Immune cells-derived secreted factors

# Cancer Microenvironment : The ECM

- The extracellular matrix (ECM): non-cellular component of tissue
- ECM is composed of and interlocking mesh of water, minerals, proteoglycans, and fibrous proteins secreted by resident cells.
- ECM is responsible for cell–cell communication, cell adhesion, and cell proliferation.

# Probing Cancer Microenvironment: The setup

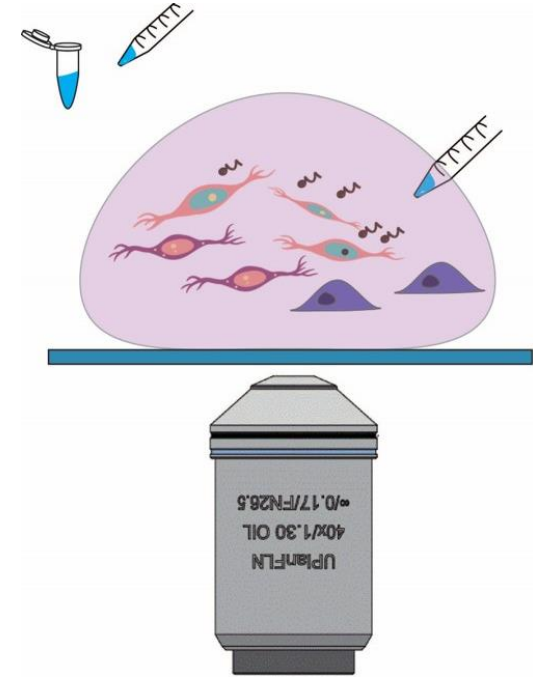
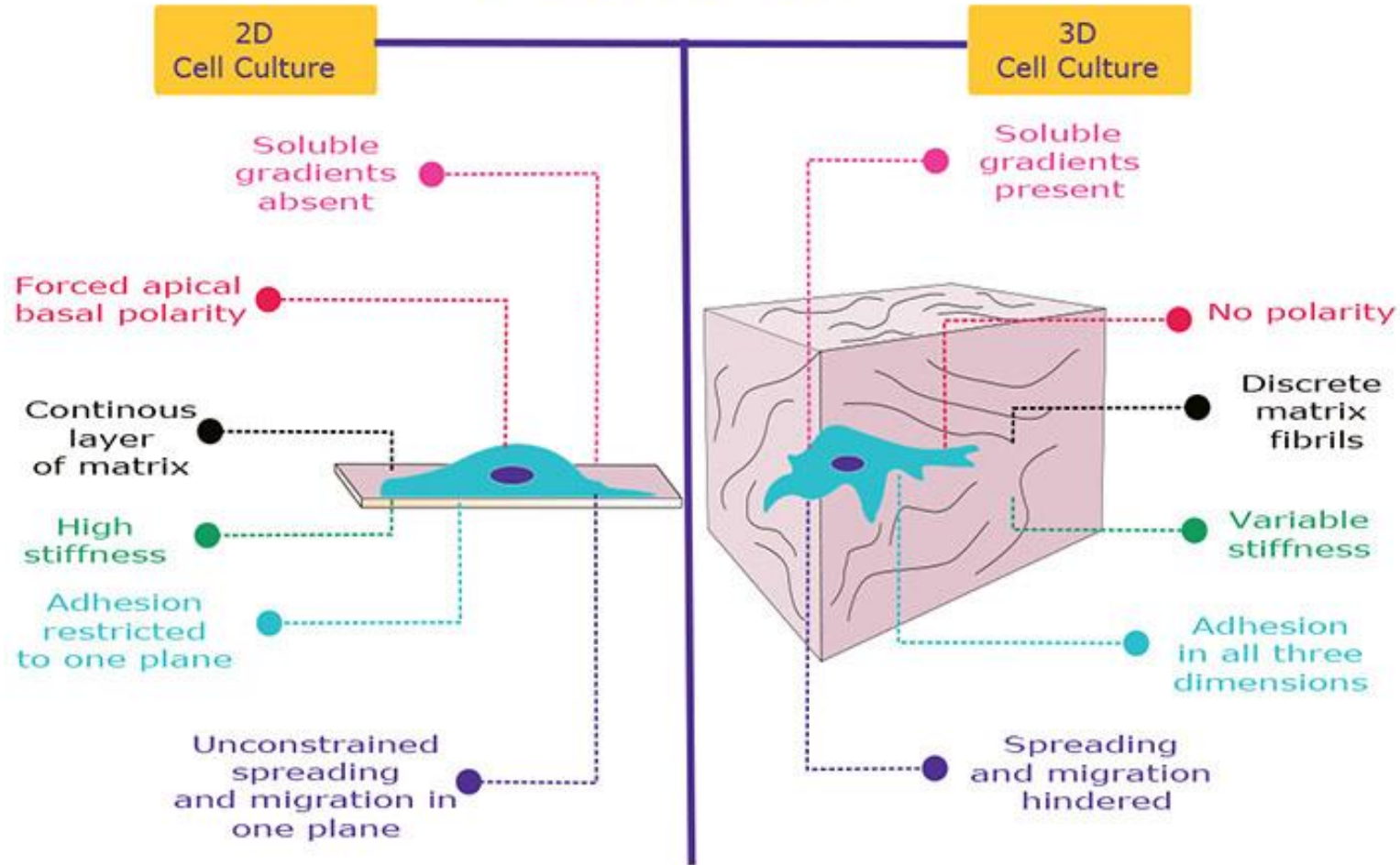


Nanomotors are injected and driven through a tumor model made by incubating cells in Matrigel droplets





# Features



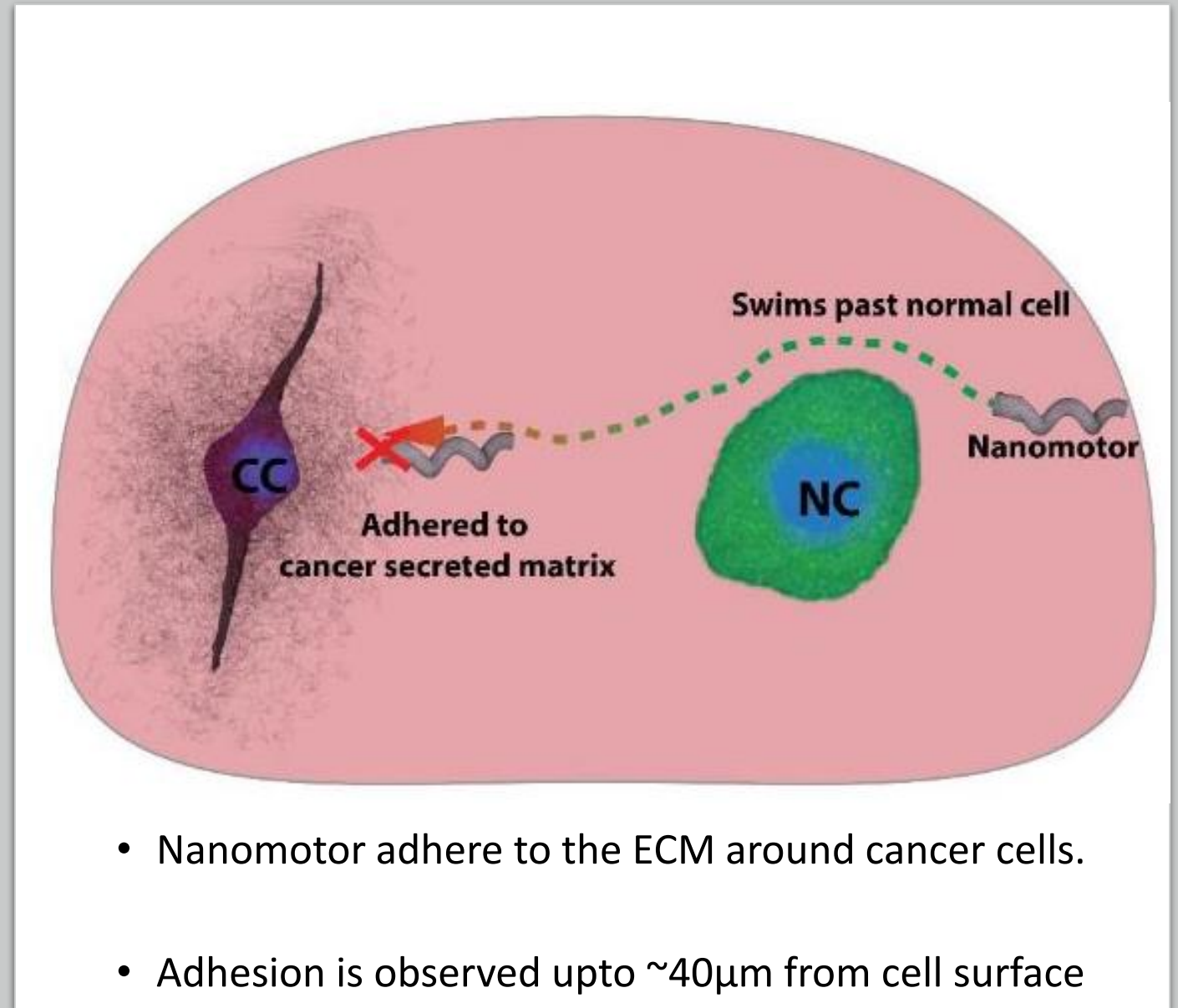
## Why 3D?



# Nanomotors adhere near cancer cells

No adhesion to **normal cell** – proximal ECM

May eventually adhere to the cell surface

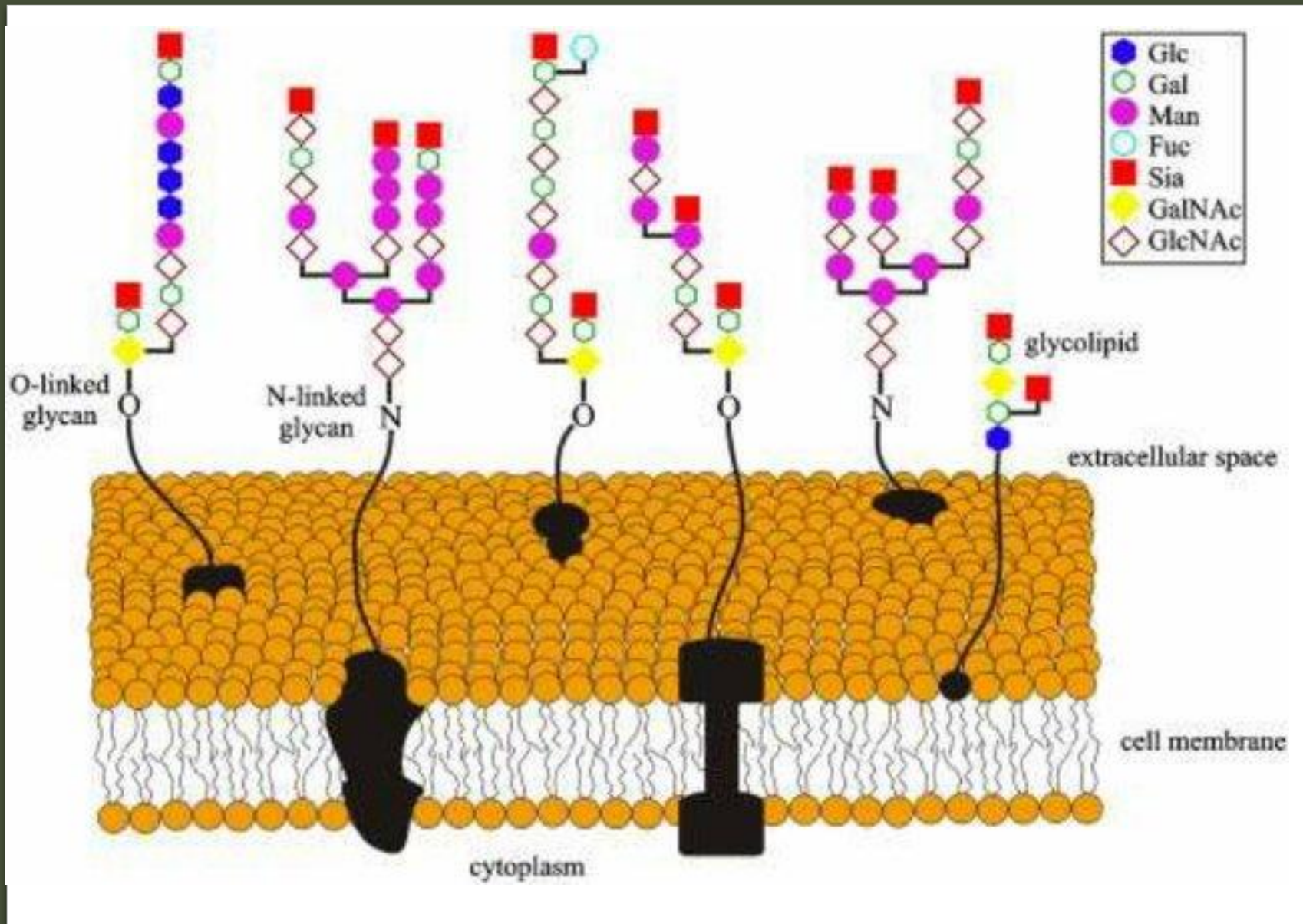


# Probing Cancer Microenvironment: Results

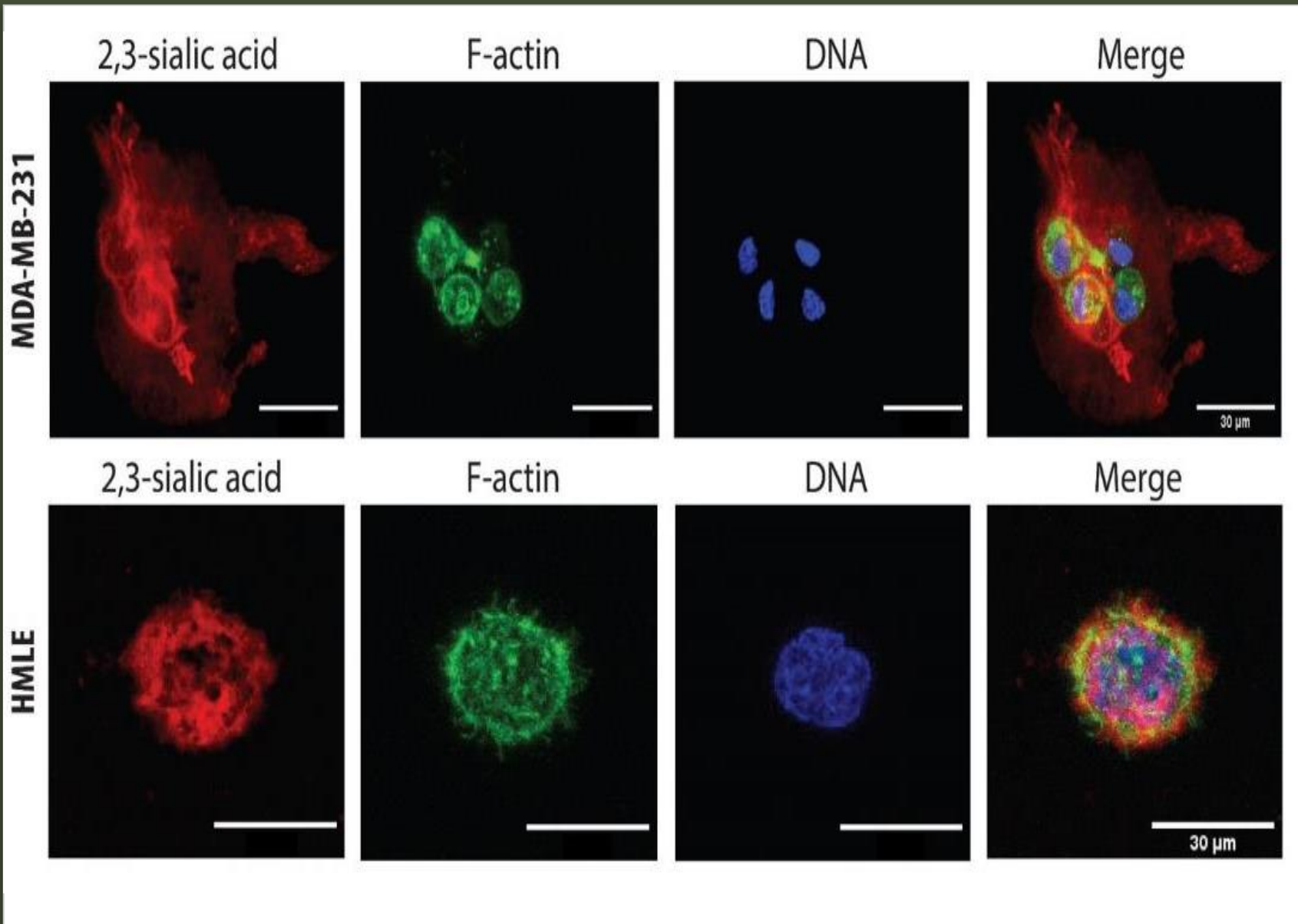
---

**Movie 1:  
Adhesion of a nanomotor  
near a cancer cell**

**Movie 2:  
No adhesion near normal  
cells at 50G, 5Hz  
Cell Type: HMLE**



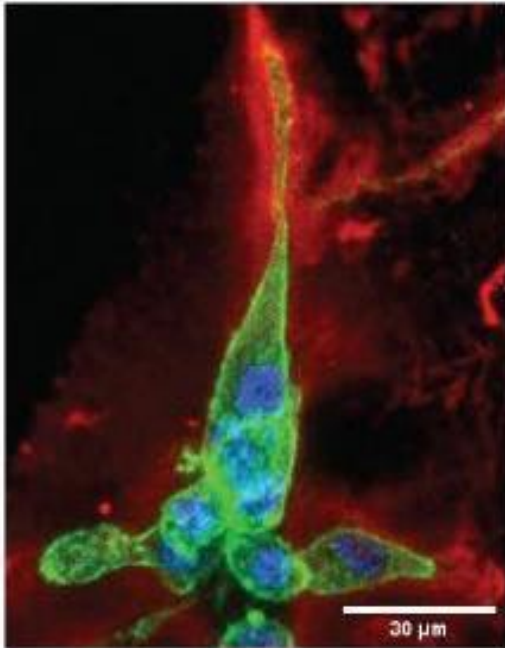
Cells secrete proteins into the ECM



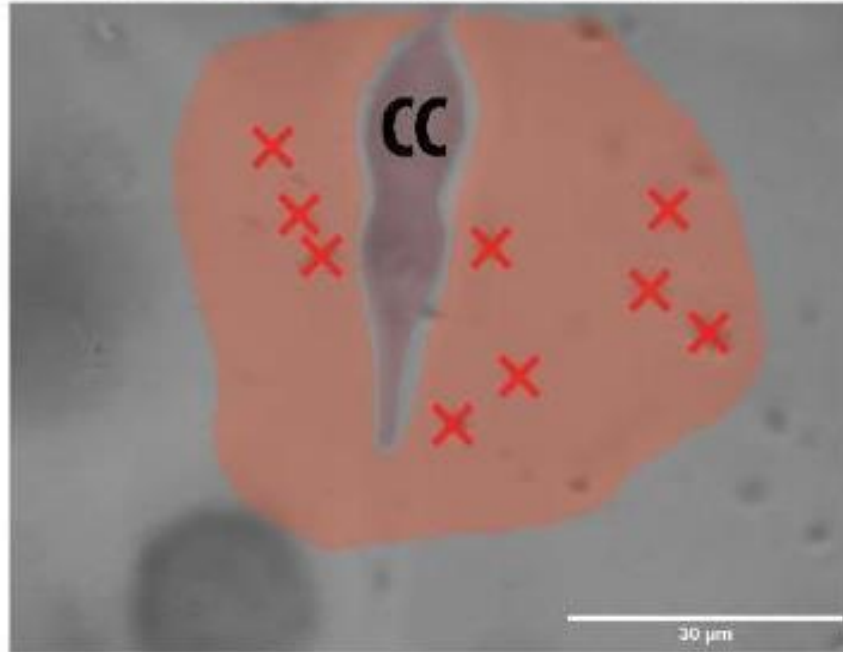
Cancer ECM  
and  
non-Cancer ECM



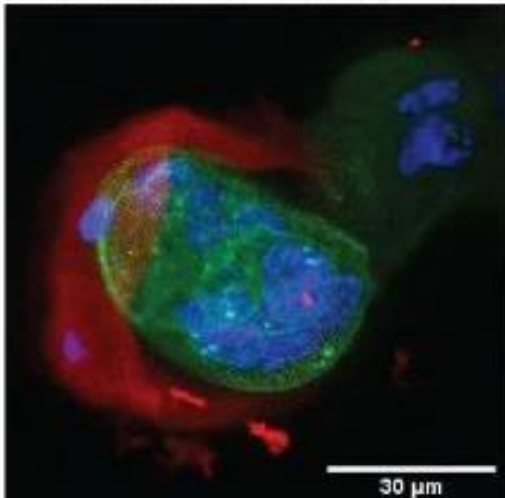
Sialic acid in MDA-MB-231



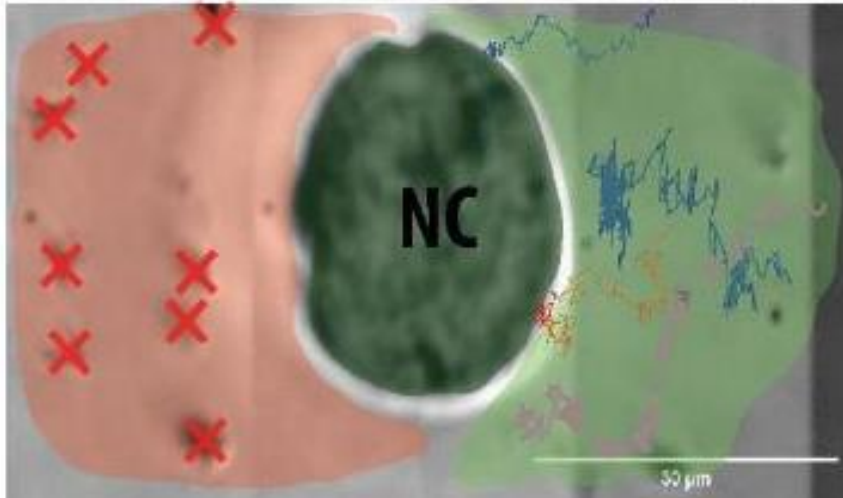
Distribution of adhered nanomotors



Sialic acid in MCF-7



Distribution of adhered nanomotors



## Cell-line specific anisotropy

Correlation between sialic acid distribution and nanomotor adhesion



**Hypersialated charged ECM secreted by cancer cells contribute to nanomotor adhesion**

# Differences in Cancer ECM and non-Cancer ECM

Surface modification of  
nanomotors using PFO

Charge shielding effect of PFO  
eliminates adhesion

**Movie 3:  
PFO coated and uncoated  
nanomotors at 150G, 3Hz**

**Cell Type: MDA-MB-231**

# Potential Applications

---

# Cancer targeting

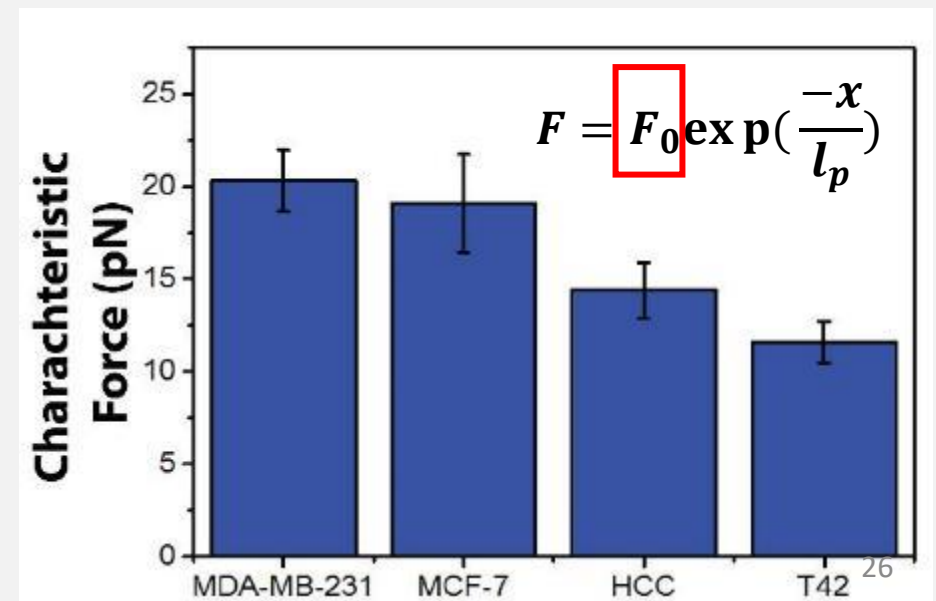
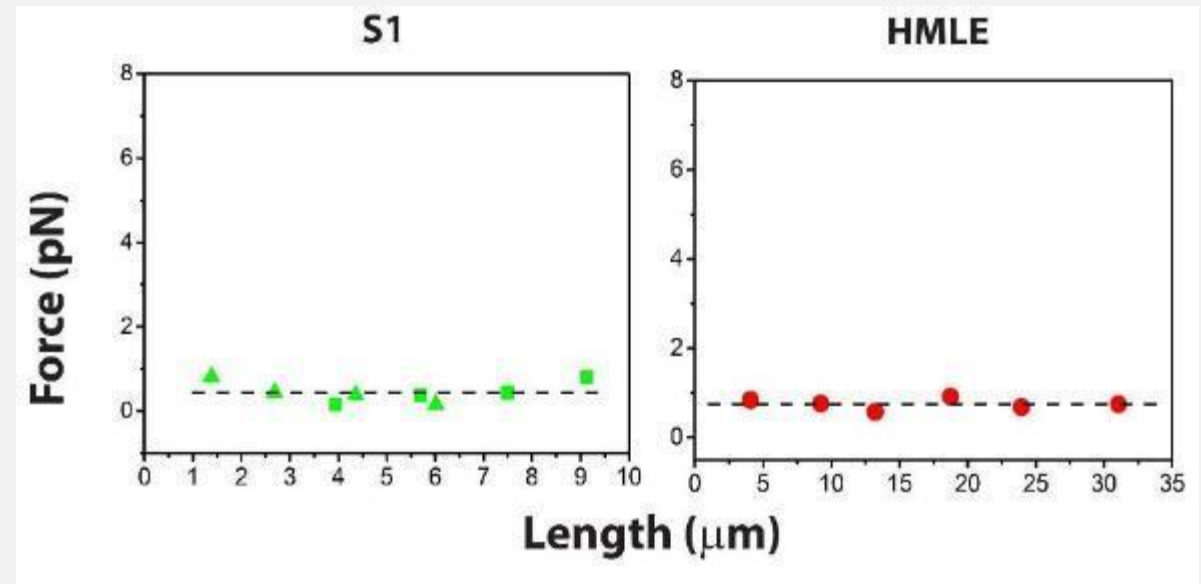
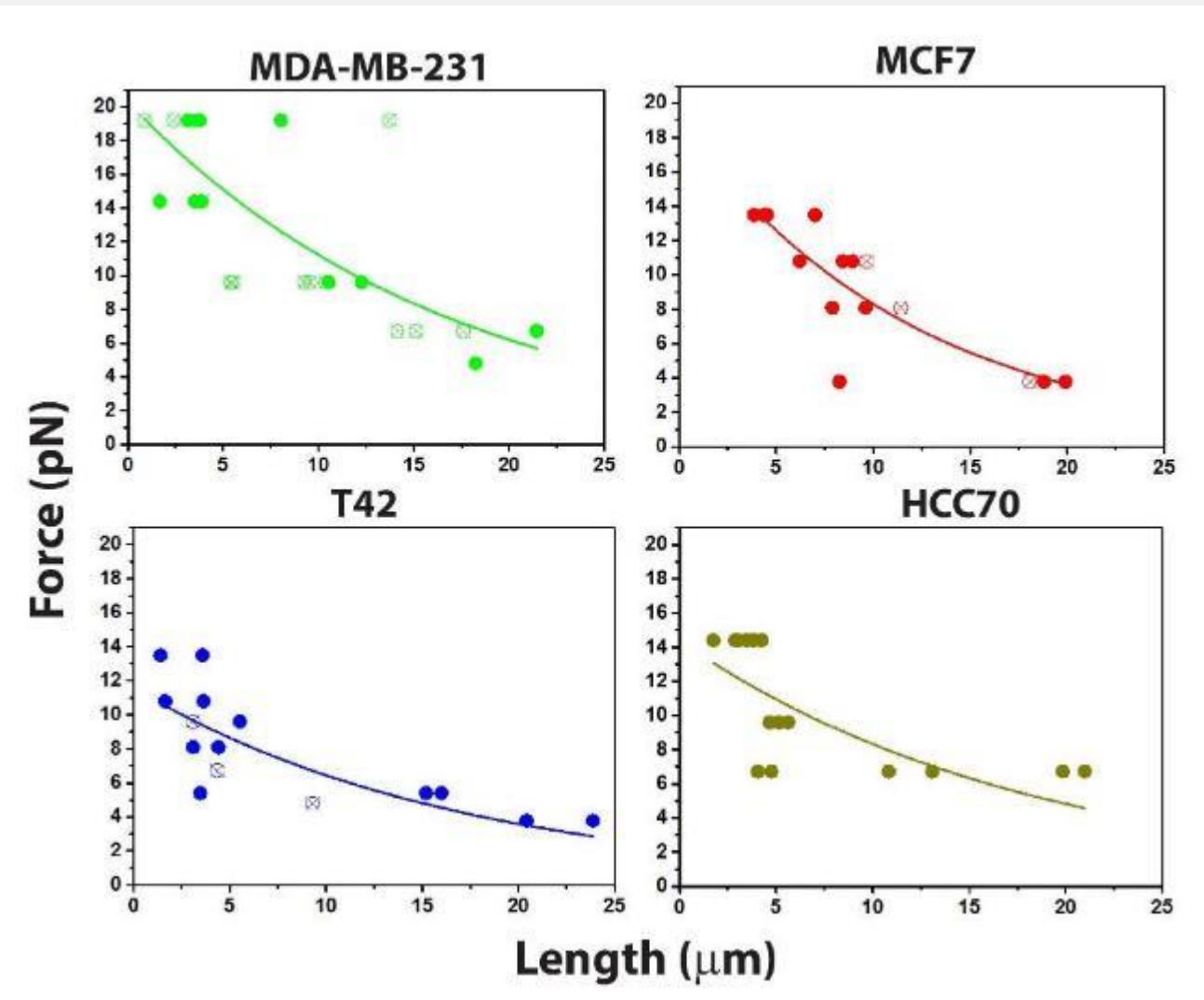
Preferential adhesion near Cancer secreted ECM can be used to target cancerous cells in a tumor

**Movie 4:  
Confocal stacks of  
co-culture in 3D matrix**

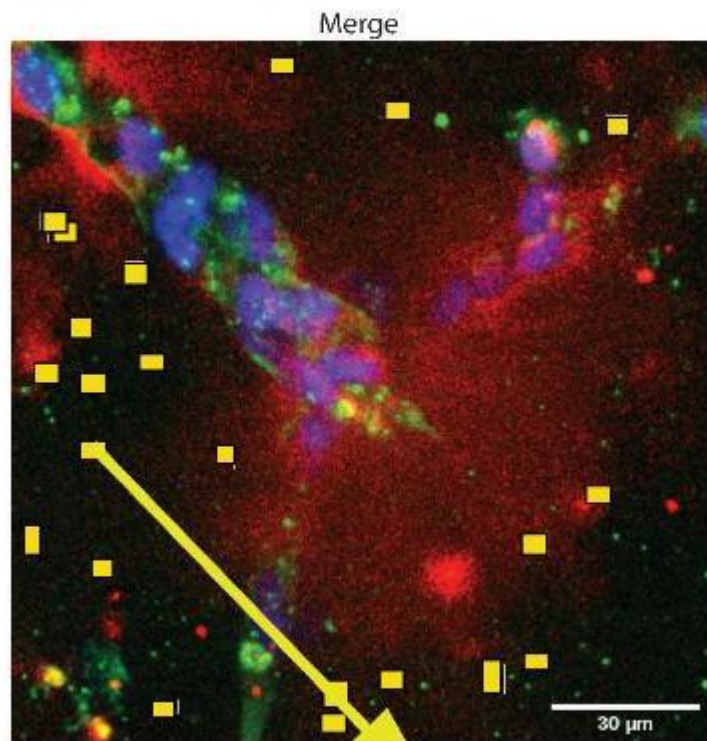
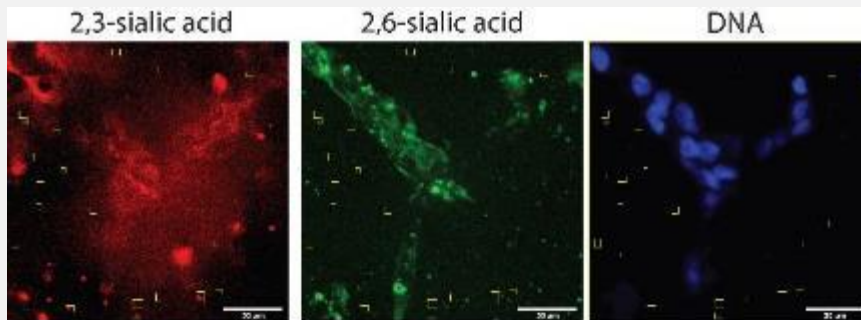
**Movie 5:  
Simulation of nanomotors  
moving through microenvironmental  
co-culture.**



# Gauging metastatic potential



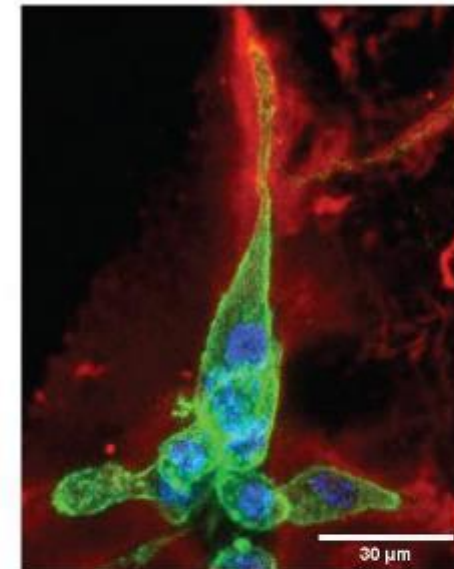
# Discovering new phenomenon



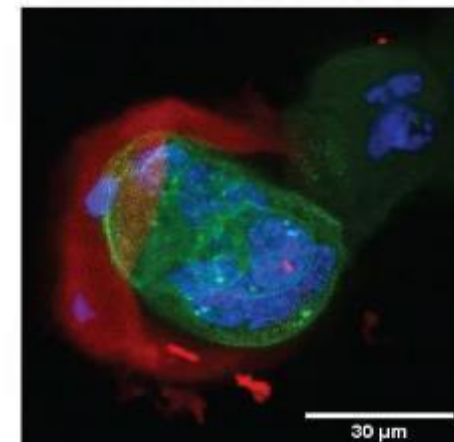
The existence of sialylated proteins in cancer-secreted ECM is reported for the first time.

Anisotropic distribution of sialylation in cancer ECM is reported for the first time.

Sialic acid in MDA-MB-231



Sialic acid in MCF-7



Micro-rheology using nanomotors

Probing the cancer microenvironment

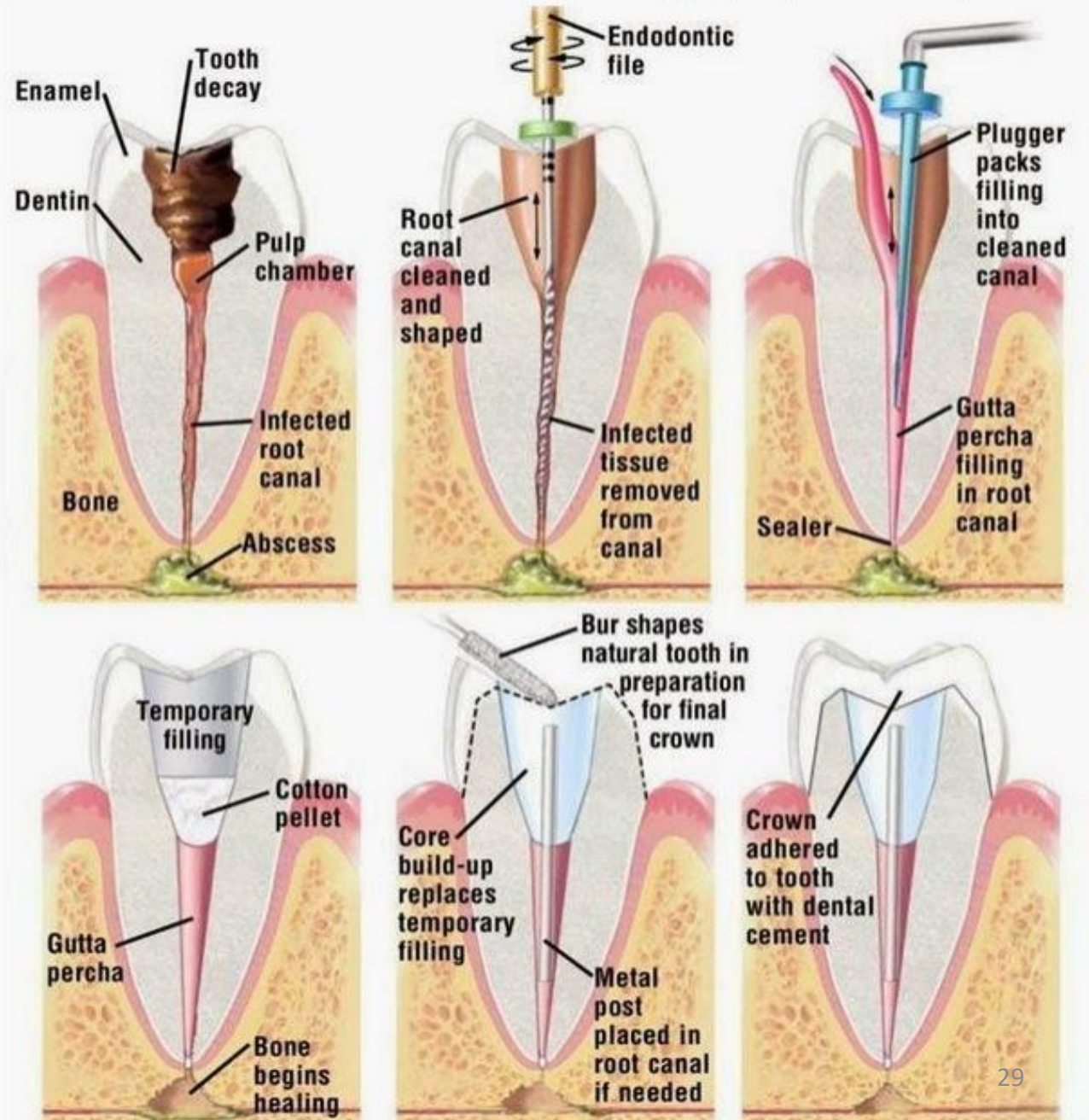
Nanomotors in real world

- Endodontic reinfection
- Problems with current treatment procedure
- Solving reinfection with nanomotors

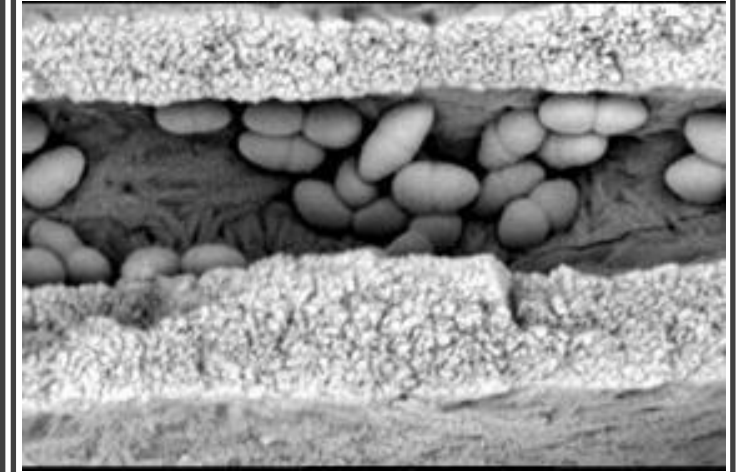
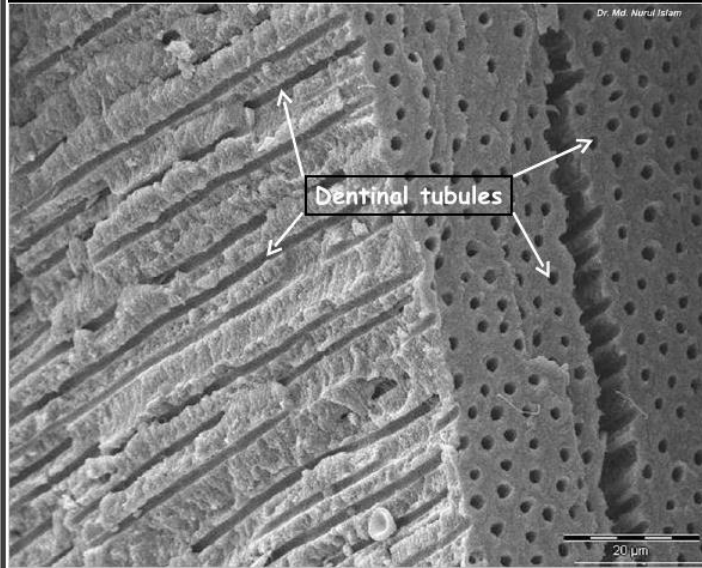
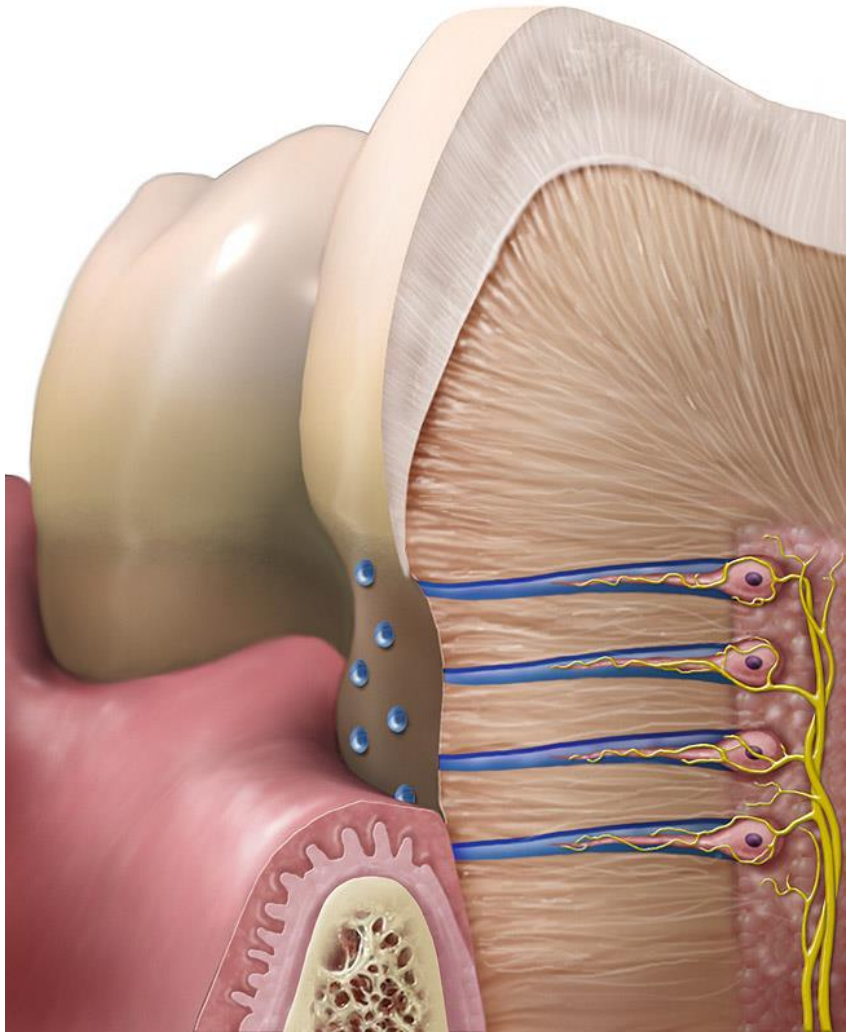


# Root canal procedure

## Root Canal Therapy (RCT)





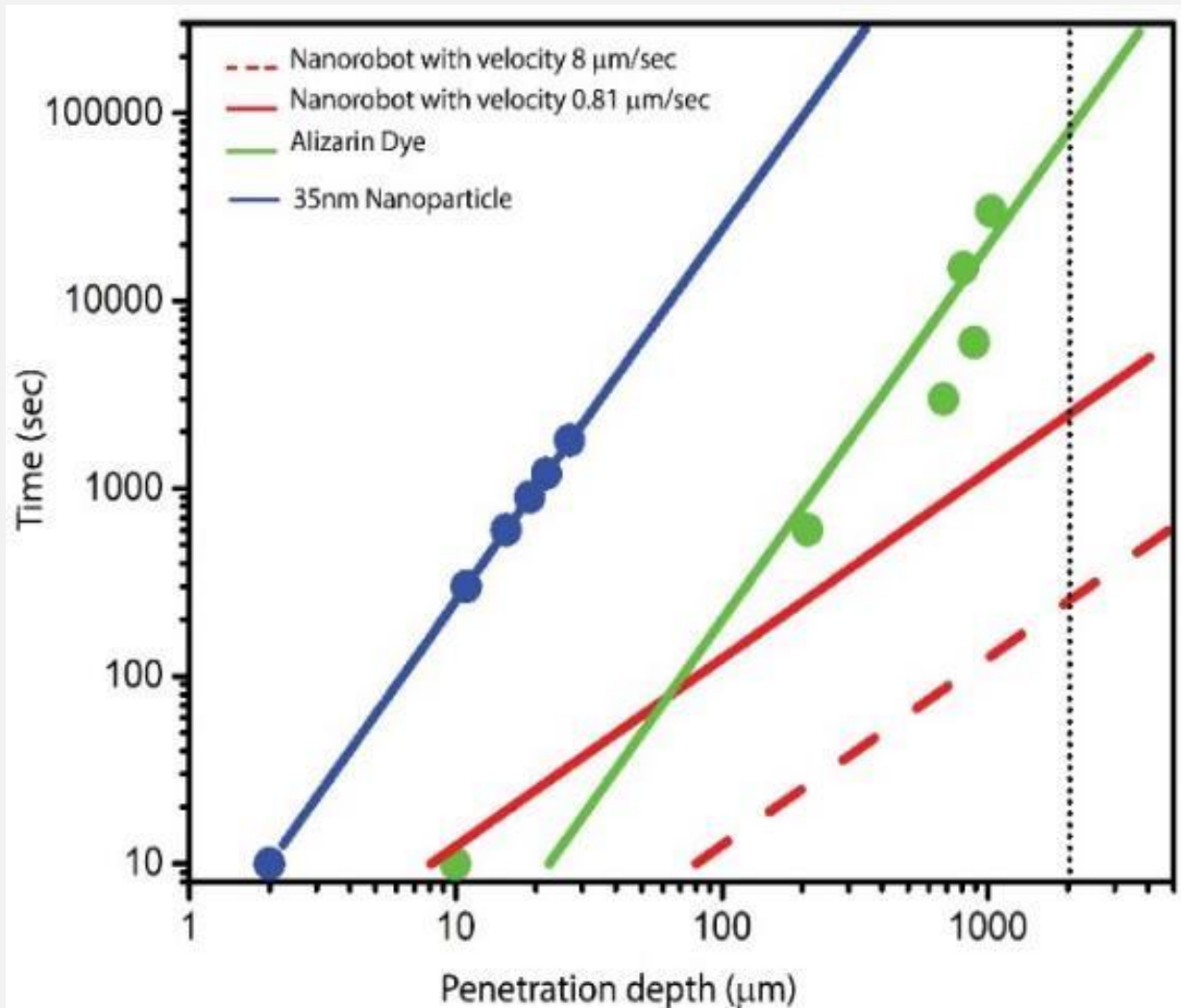


# Endodontic Reinfection

---

# Limitations of current technology

## Relying on diffusion alone is hopeless



## Currently available devices



LASER

**Fotona**  
Ultra Performance Lasers™

Depth inside Dentinal Tubules

500μm – 850μm



Ultrasound

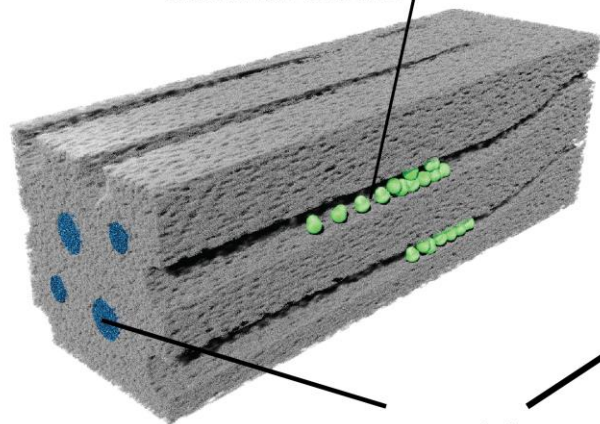
**SybronEndo**  
Dentsply  
Sirona

100μm – 250μm

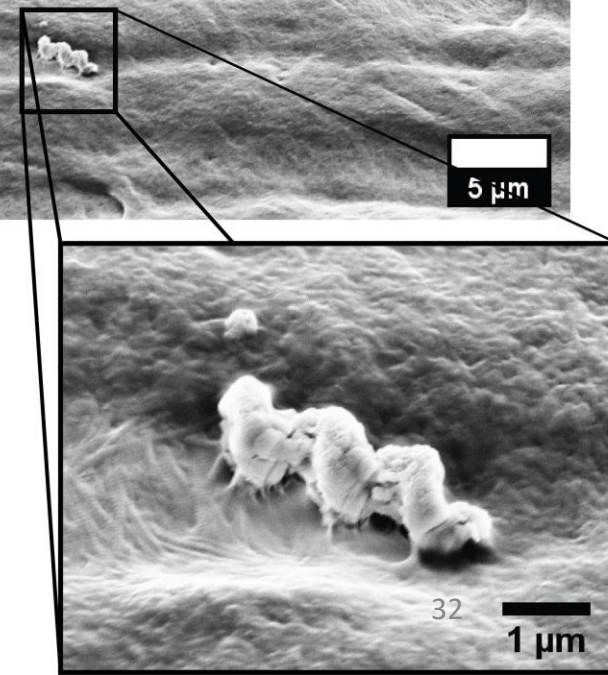
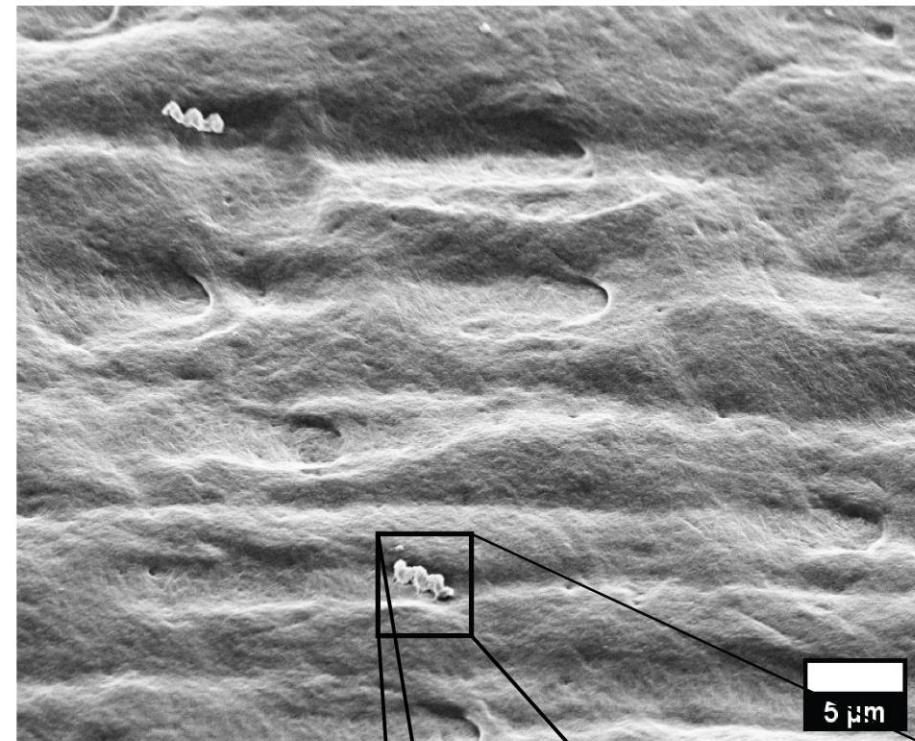
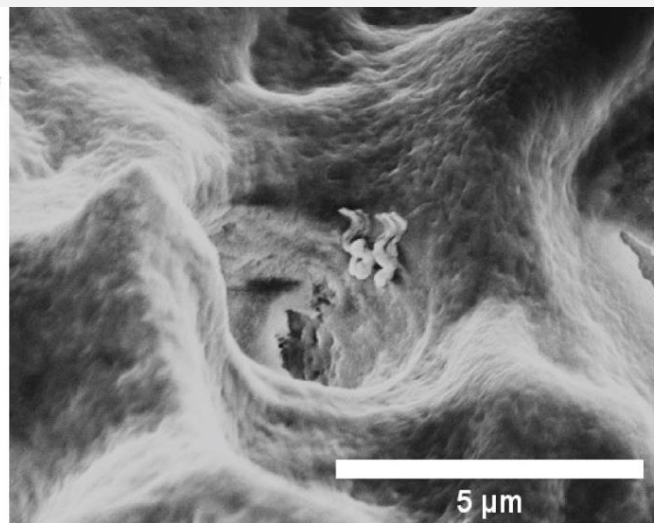
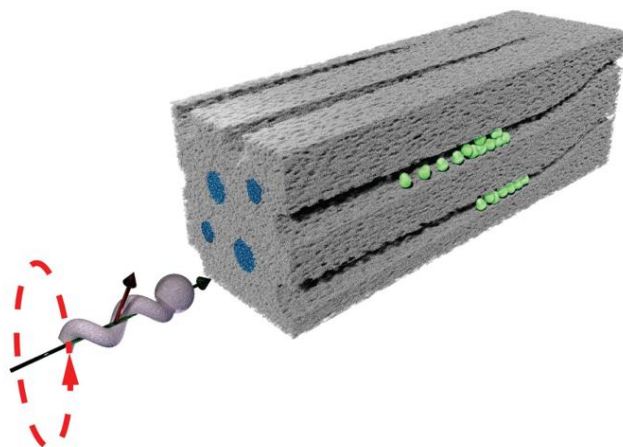
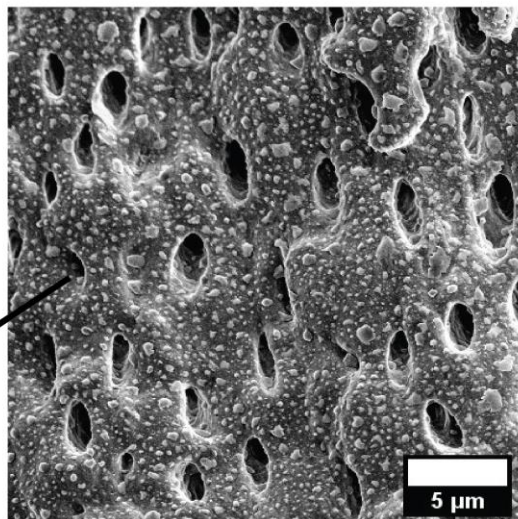


# Our solution

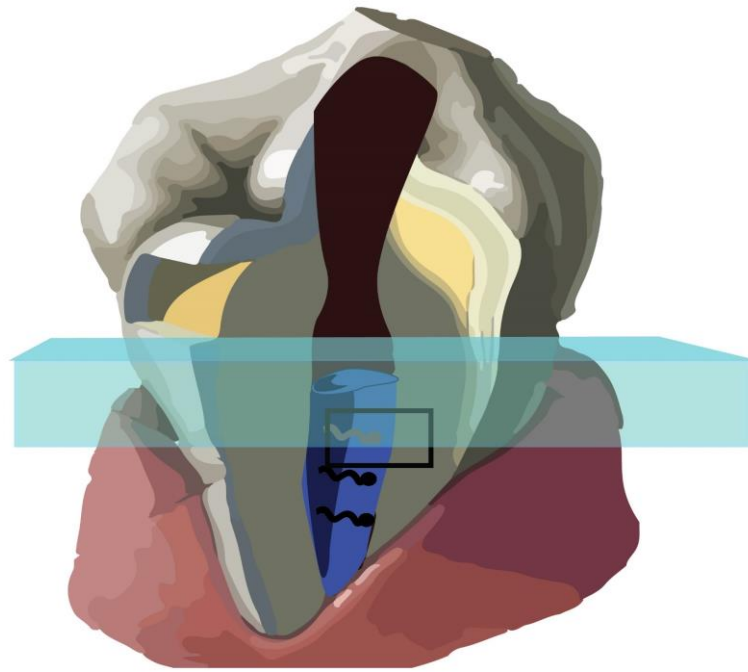
Bacterial colony inside a dentinal tubule



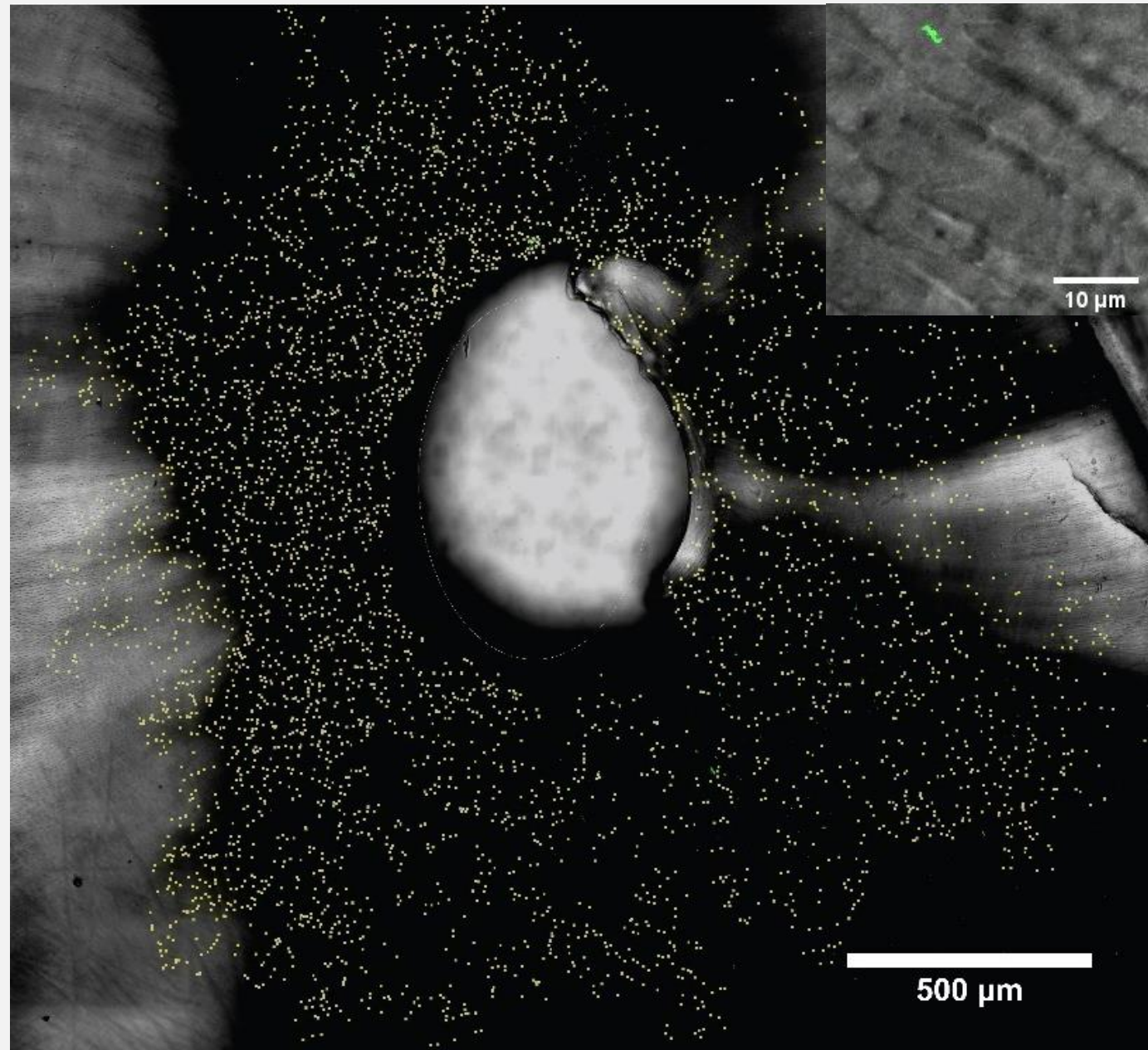
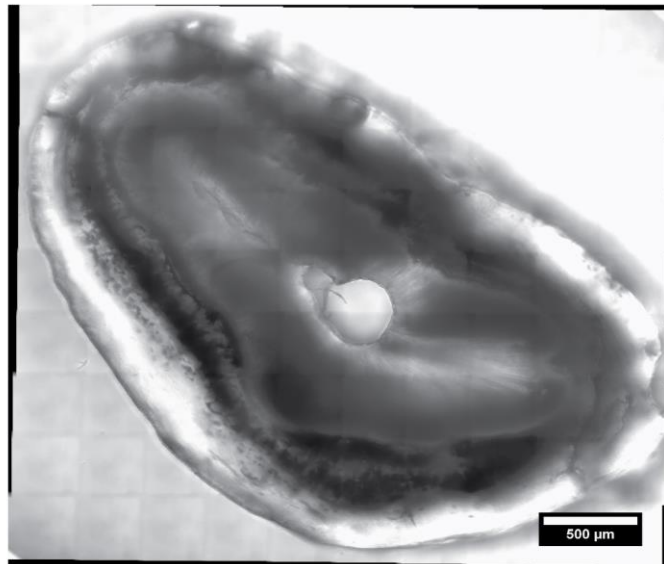
Entrance of dentinal tubules





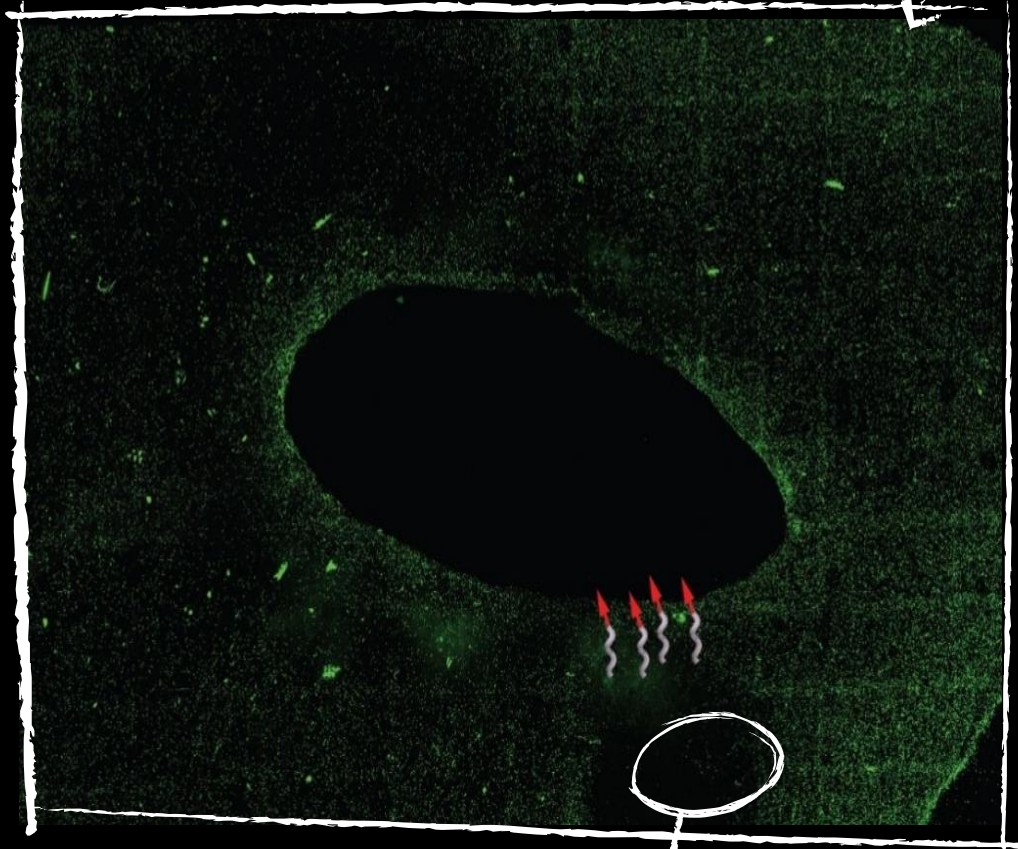


Cross section of human teeth used for experiments

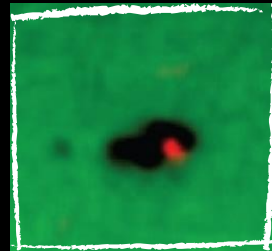




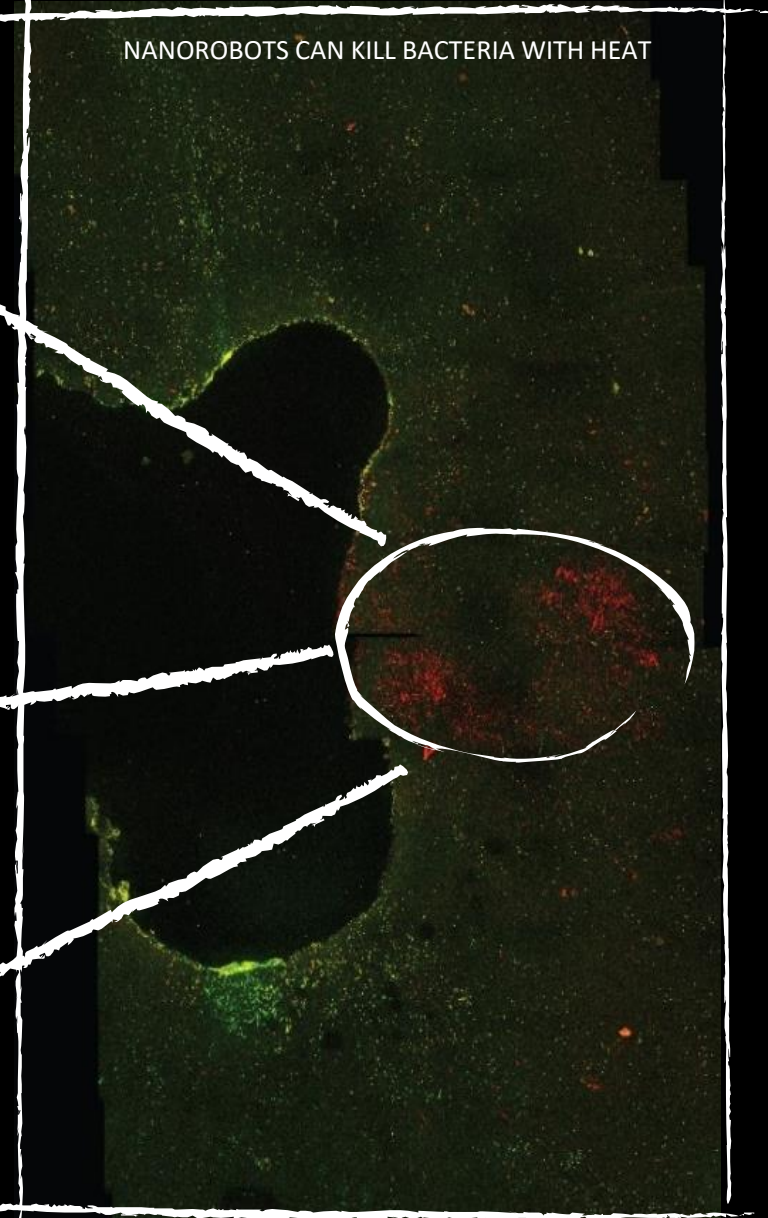
NANOROBOTS CAN BE RETRIEVED WHEN THE JOB IS DONE



Area of retrieved Nanorobots



NANOROBOTS CAN KILL BACTERIA WITH HEAT





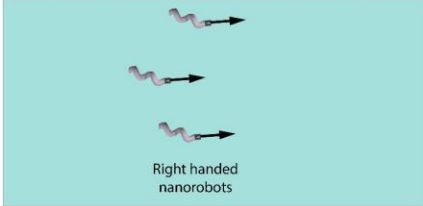
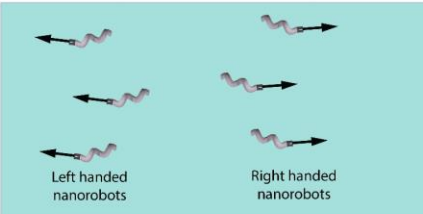
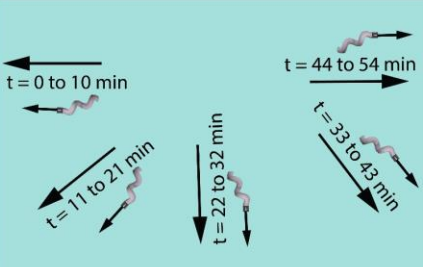
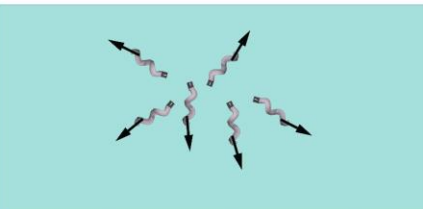
# Publications

- Helical Nanomachines as Mobile Viscometer,  
**Advanced Functional Materials**, 1705687, 2018
- Helical nanobots as mechanical probes of intra- and extracellular environments  
**Journal of Physics: Condensed Matter**, 224001, 2020
- Nanomotors Sense Local Physicochemical Heterogeneities in Tumor Microenvironments\*\*.  
**Angewandte Chemie - International Edition (2020)**  
**doi:10.1002/anie.202008681.**
- Nanomotors for treatment of endodontic reinfection  
**D. Dasgupta\***, S. Srinivas\*, A. Ghosh  
*Chemrxiv*

Thank You

# EXTRAS

# Treating Endodontic Reinfection: Comparison

Unidirectional rotating field Single Chirality	Angular Distribution	Area of sector of dentin covered	Experimental time needed to achieve area coverage	Comments
 <p>Right handed nanorobots</p>	Gaussian with single peak and FWHM $\sim 40^\circ$	$\sim 11\%$	20 minutes	Precisely targeted penetration in one sector of the dentine
<p>Unidirectional rotating field Opposite Chirality</p>  <p>Left handed nanorobots      Right handed nanorobots</p>	Bimodal FWHM $\sim 50^\circ$	$\sim 28\%$	20 minutes	Precisely targeting diametrically opposite sectors of the dentine
<p>Rotating rotating field</p>  <p>t = 0 to 10 min      t = 44 to 54 min t = 11 to 21 min      t = 33 to 43 min t = 22 to 32 min</p>	Uniform distribution	$\sim 100\%$	120 minutes	Uniform sector by sector delivery in dentine
<p>Oscillating field</p> 	Uniform distribution	$\sim 100\%$	20 minutes	Uniform one shot delivery in dentine

magnetic torque on the helix due to the rotating magnetic field is denoted by  $\tau$ . The dynamics of the helix can be written as:  $\tau = \gamma\omega$  where  $\gamma$  is the rotational friction tensor and  $\omega$  is the angular velocity vector. The torque is related to the magnetic moment  $m$  and  $B$  as:  $\tau = m \times B$ .

The magnetic field in the body frame ( $x'y'z'$ ) of a helix is related to a magnetic field rotating in

the lab frame by the following equation:  $\begin{bmatrix} B_{x'} \\ B_{y'} \\ B_{z'} \end{bmatrix} = R \times \begin{bmatrix} B \cos(\Omega_B t) \\ B \sin(\Omega_B t) \\ 0 \end{bmatrix}$ , where  $R$  is the

transformation matrix and  $t$  is the time elapsed. The body frame magnetic field may be used to

derive the body frame torque:  $\begin{bmatrix} \tau_{x'} \\ \tau_{y'} \\ \tau_{z'} \end{bmatrix} = \begin{vmatrix} \vec{i} & \vec{j} & \vec{k} \\ m \cos \theta_m & 0 & m \sin \theta_m \\ B_{x'} & B_{y'} & B_{z'} \end{vmatrix}$  where  $m$  is the magnetic

moment projected along the long axis and short axis.

Using standard notations to represent the Euler angles to describe the generalized orientation of a symmetric elongated object we can obtain the angular velocities in the

body frame which are:  $\omega_{x'} = \dot{\phi} \sin \theta \sin \psi + \dot{\theta} \cos \psi$ ,  $\omega_{y'} = \dot{\phi} \sin \theta \cos \psi -$

$\dot{\theta} \sin \psi$ ,  $\omega_{z'} = \dot{\phi} \cos \theta + \dot{\psi}$ .

Equating the two expressions for the torque and solving for  $\dot{\phi}$ ,  $\dot{\psi}$ ,  $\dot{\theta}$ , we get the Euler

equations with  $\beta = \Omega_B t - \phi$ :

$$\dot{\phi} = \frac{mB}{\gamma_s \sin \theta} (\sin \theta_m \cos \beta + \cos \theta_m \sin \beta \sin \theta \cos \phi)$$

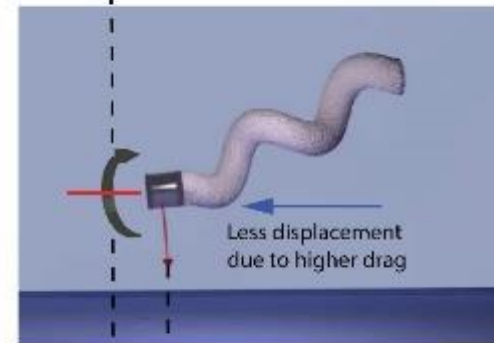
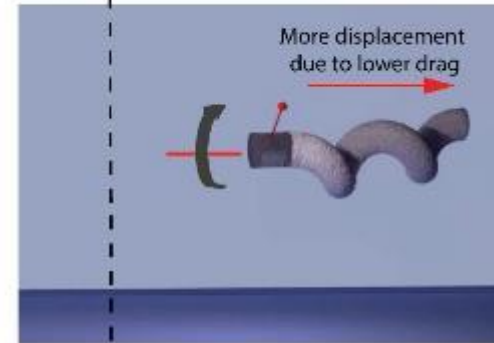
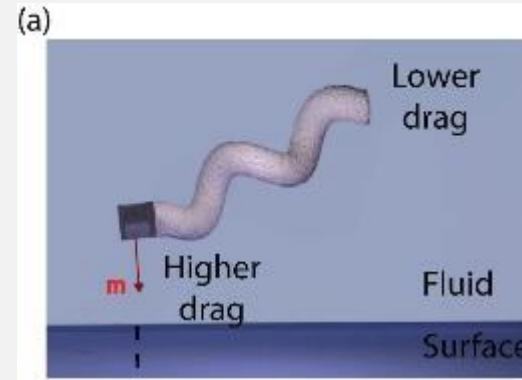
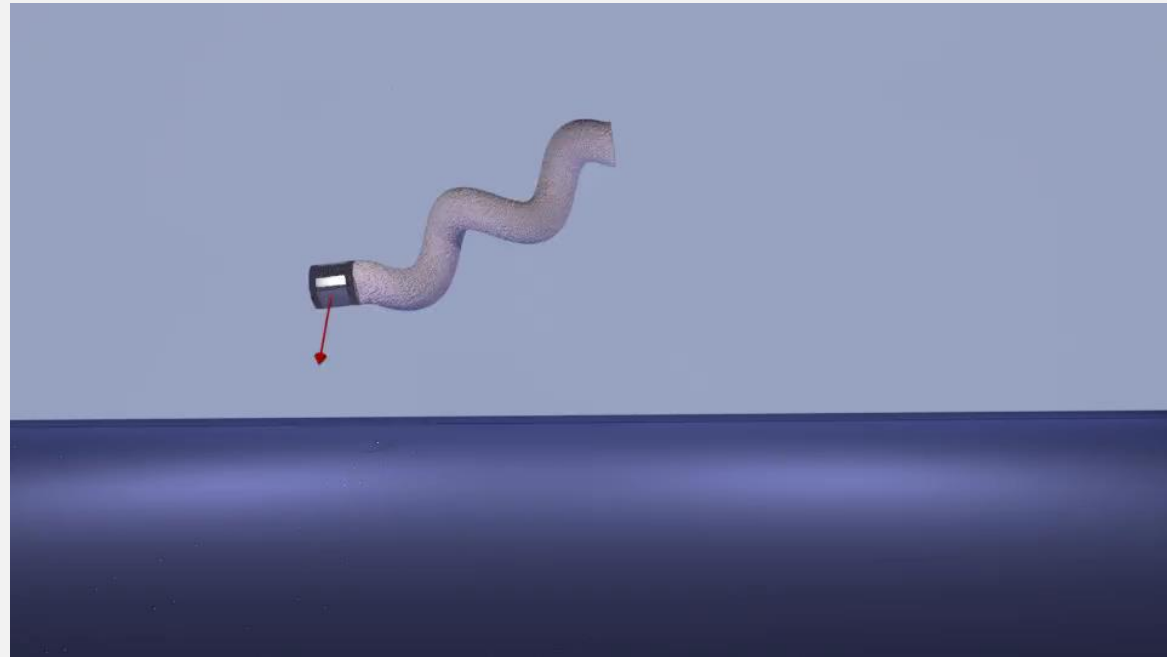
$$\dot{\theta} = -\frac{mB}{\gamma_s} \sin \beta (\sin \theta_m \cos \theta + \cos \theta_m \sin \theta \sin \psi)$$

$$\dot{\psi} = \frac{mB \cos \theta_m (\sin \beta \cos \theta \cos \psi - \cos \beta \sin \psi)}{\gamma_l} - \dot{\phi} \cos \theta$$

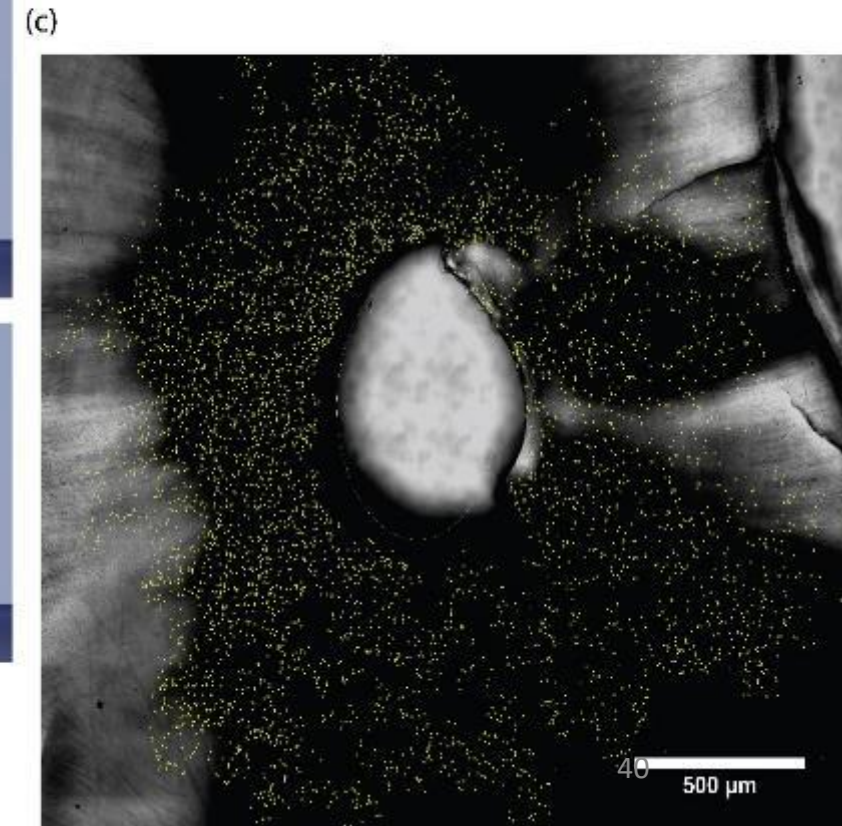
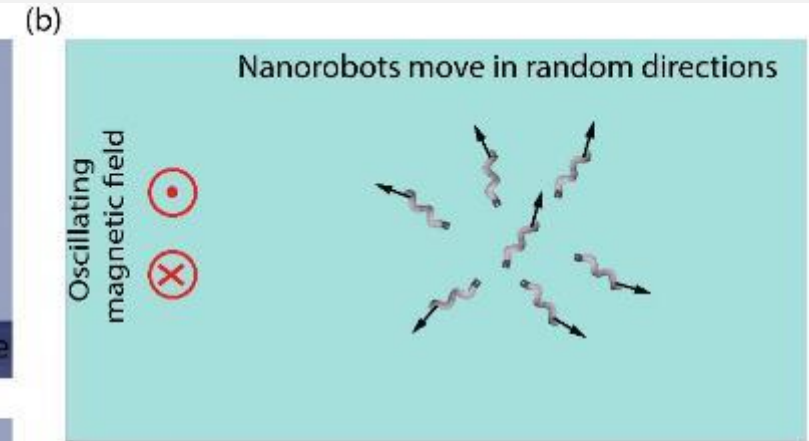
The above equations can be solved for the steady state configurations where  $\theta$  and  $\psi$  remain constant in time. This leads to two different dynamical configurations for an object rotated by an external torque namely 'tumbling' and 'precession'. Tumbling motion means a precession angle  $\theta = 90^\circ$ . This occurs for all frequencies below  $\Omega_1$  denoted by  $mB/\gamma_s$ . At very low actuating frequencies ( $\Omega_B < \Omega_1$ ), the magnetic moment of the nanomotor can follow the applied magnetic field with a constant phase difference and hence a phase locked tumbling motion of the nanomotor is observed, i.e., the nanomotor shows rotation about its geometric short axis. Above  $\Omega_1$ , the nanomotor starts to precess about the axis of rotating field. This happens because beyond this frequency the angle between  $m$  and  $B$  becomes more the  $90^\circ$  and the moment can no longer follow the magnetic field, thus causing phase slip. Precessional motion ( $\theta < 90^\circ$ ) is a solution to the Euler angles and the object can show precessional phase locked motion for  $\Omega_B > \Omega_1$ . Above the critical frequency  $\Omega_2$ , the magnetic moment of the helix starts to phase slip with the magnetic field.



# Treating Endodontic Reinfection: Oscillating field



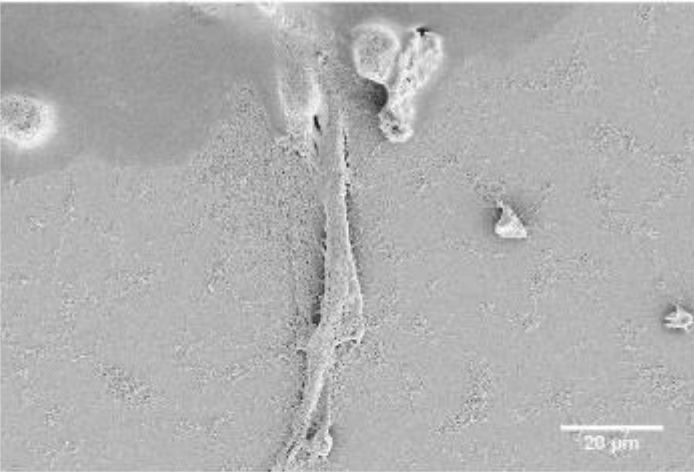
Effective displacement  
for 1 oscillation



# Differences in Cancer ECM and non-Cancer ECM

Physical differences

MDA-MB-231



HMLE

